

University of Milan
Department of Biomedical Sciences for Health

Ph.D in Morphological Sciences

XXVIII cycle

**THE PEDIATRIC FLAT FOOT:
PRE AND POST SURGICAL CORRECTION
3D KINEMATICS DATA**

Coordinator: Prof. Virgilio F. Ferrario

Artemisia Panou, M. D.

Register number: R10229

Tutor: Prof.ssa Chiarella Sforza

Co-tutor: Prof. Nicola Portinaro

*To the people who have indelibly marked my life:
Kostantinos, Dimitris, Lida, Nicola and Andrea*

ABSTRACT

Introduction: aim of this study was to establish normality parameters and analyze 3D kinematic data before and after surgical correction of the pediatric flexible flat foot

Materials and methods: study population was composed of 2 groups: 10 children (20 feet, 5M/5F) without any disorders of the foot were evaluated to obtain normal reference data; 20 children with bilateral flexible flatfoot candidate to bilateral surgical correction (40 feet, 13M/7F) The RFM -3D kinematics protocol was used. Clinical, radiographic and instrumental evaluation were performed preoperatively and at 12 months by the same surgeon An arthroereisis of the subtalar joint was performed by the same surgeon. Patients were divided in 3 groups: 1: normality; 2: before surgery; 3: after surgery. For all the variables and for the three planes of the space comparison between groups were performed.

Results: 3D rotational joint variables and planar angles were defined for normality, before and after surgery at the upright standing position. Differences were observed: hind foot, frontal plane; Chopart Joint, transverse plane; Lisfranc Joint, frontal/transverse planes; ratio between 1st and 2nd metatarsal, transverse plane; 2nd and 5th metatarsal versus ground respectively, sagittal plane; MLA, transverse plane

Discussion/conclusions: different variables, normalized after correction, suggest that surgery performed at the hind foot can also improve mid foot pronation, increase the medial longitudinal arch and improve ratio between metatarsal bones, allowing to quantify changes that clinical and radiological evaluation cannot provide. The pediatric foot is similar to the adults and pediatric flexible flat foot could be corrected surgically, even if painless.

TABLE OF CONTENTS

ABSTRACT	3
TABLE OF CONTENTS	4
PART 1: FOOT AND GAIT ANALYSIS.....	6
INTRODUCTION.....	7
History of gait analysis	7
THE MOTION	13
The gait cycle.....	13
Characteristics of the gait: cadence, average speed and stride length.....	14
Phases and events of the normal human gait	14
Sequence of the muscle activity during gait	19
Specificity of the gait in childhood.....	20
METHODS TO STUDY THE MOVEMENT	23
Kinematics	24
Optical Systems	24
Optoelectronic optic systems	25
Kinetics	26
Surface Electromyography.....	30
The study of human movement: an overview	31
Study of treadmill gait	31
THE FOOT.....	33
The morphogenesis of the foot.....	33
Anatomy and biomechanics of the foot and ankle	34
PART 2: THE PEDIATRIC FLAT FOOT, PRE AND POST SURGICAL CORRECTION 3D KINEMATICS DATA	43
INTRODUCTION.....	44
The pediatric foot.....	46
MATERIALS AND METHODS	47
The Rizzoli Foot Model.....	47

Modification of the original RFM.....	50
Inclusion and exclusion criteria	52
Clinical and instrumental assessment	53
Surgical Technique	54
Statistical analysis of the data	56
RESULTS.....	56
Definition of normality values	56
Kinematic data before and after surgical correction of the foot, at the static upright position.....	60
DISCUSSION	67
Definition of normality parameters.....	68
Comparison between normality, before and after surgery	68
CONCLUSIONS	69
REFERENCES.....	71

PART 1:
FOOT AND GAIT ANALYSIS

INTRODUCTION

History of gait analysis

For all people born in the 20th century it may seem simple to observe recordings or live shots of the human body in motion. Cinema and, after the 50^s, television and computers have made quite common to observe and film moving objects, including human motion. These resources allow us to "capture" a phenomenon intrinsically connected to the concept of our life. Furthermore, until the end of the 19th century, there was no direct way to describe movement, except through imagination evoked by verbal description and literature, painting or music. In the 19th century, photography has expanded the horizons of pictorial representation. However, a more important revolution was the one given by cinematography, officially born on December 28th 1895 by Lumière brothers (Figure 1) and developed in the 20th century. Cinematography offered the possibility to observe humans movement, influencing irreversibly science and art.



Figure 1 Lumiere Brothers: Auguste (1862-1954) and Louis (1864-1948)
source: <http://www.institut-lumiere.org/francais/patrimoinelumiere/brevehistoire.html>

Science was always attracted by human motion long before the arrival of cinematography. An important primacy should be recognized to Giovanni Alfonso Borelli, who in 1682 published the famous "*De Motu Animalium*" (Figure 2) and also described the head movements and the balance maintenance during motion, according to the known laws of mechanics of his era [1].

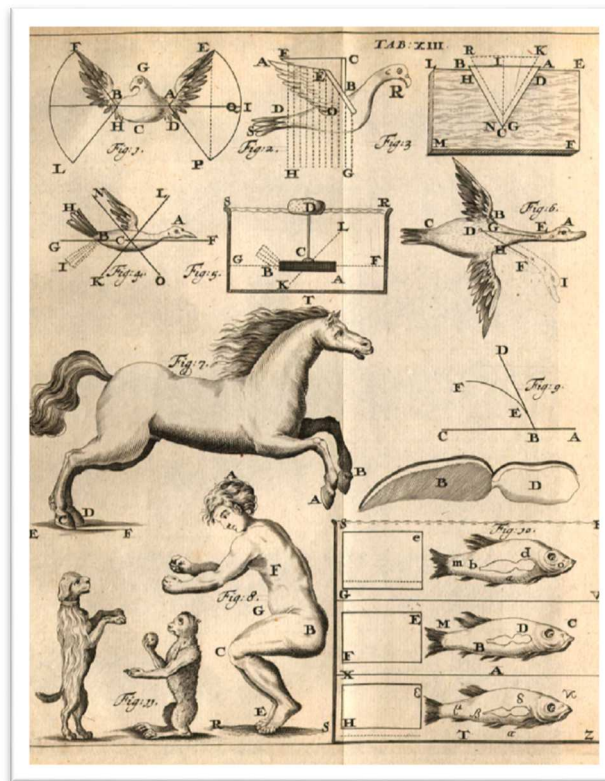


Figure 2 De Motu Animalium" - Borelli Giovanni (Rome: A. Bernabo, 1680)

The first description of the multi-factorial gait cycle is attributed to Ernst Heinrich Weber (1795-1878) and his two brothers Eduard (1804-1891) and Friedrich Wilhelm (1806-1871). The subject of their several experiments was the study of the bony lever arms and the length of the muscles during their contraction. They described the changes in stride length and cadence in relation to different walking speeds. Moreover, they studied the function of the ligaments, the displacement of the body centre of mass during walking and the pendulum motion of the lower limbs [2].

Etienne Jules Marey (1830-1904) studied the animal movement in many of its variants and his opera "*La machine animale, locomotion terrestre et aérienne*" (1873), is a milestone in the history of the physiology of human movement. The detailed study of the movements pushed Marey to invent several instruments such as the chronophotographer, the photographic gun, as well as the first film-camera. The film is the most common support in all-photographic applications, until the recent development of digital photography [3].

In the second part of the 19th century, advances in the study of the movement have had a major boost thanks to a curious cultural debate born in the United States. The theme was the most used mean of locomotion in human history: the horse. The discussion centred on "canter" (gait characteristic of semi-canter) and the question was about the existence or not of a phase of full suspension respect to the ground. An eccentric patron of the United States promised a high money prize to whom for first would be able to

prove how things were exactly. The prize was won by another very eclectic character, the American Eadweard Muybridge (1830-1903). Muybridge had developed the technique of Marey's chronophotography: he started a series of pictures of animals and humans movement, during their multiple activities, obtained in a rapid sequence (about 5 for second). Finally, in 1878 he was able to capture, in the famous series of photographs entitled "*The Horse in Motion*", the moment when during the "canter" all the horse's legs were lifted up from the ground (Figure 3) [4].

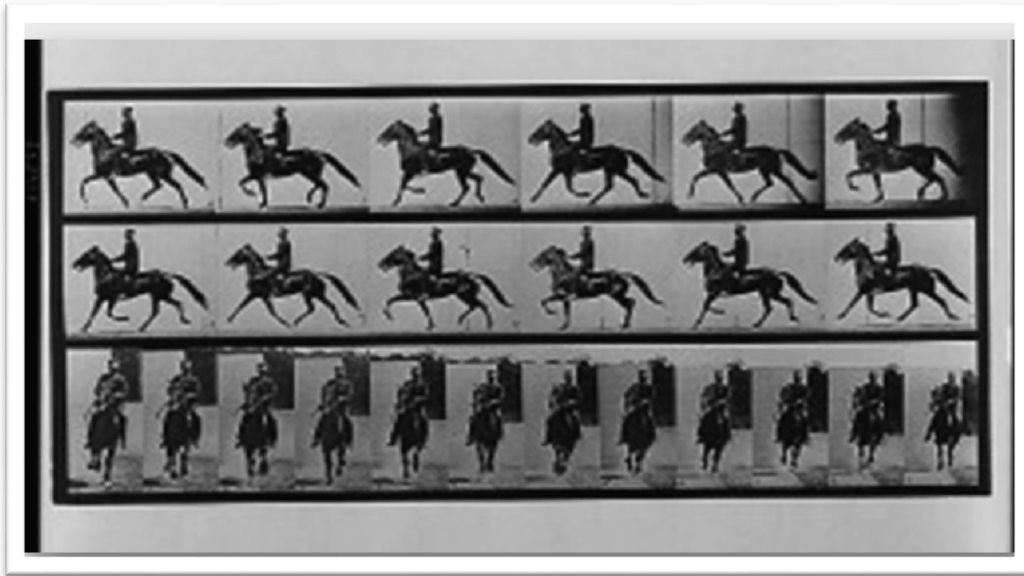


Figure 3 Animal locomotion by Eadweard Muybridge (Philadelphia, Photogravure Company of New York, 1887, pl. 593)

Muybridge's work had an important impact in two contexts, apparently far away from each other: the scientific and the artistic, including the human portraiture (Figure 4). Movement could be considered "captured" as a sequence or as an overlay of images, each of them static in itself [4].

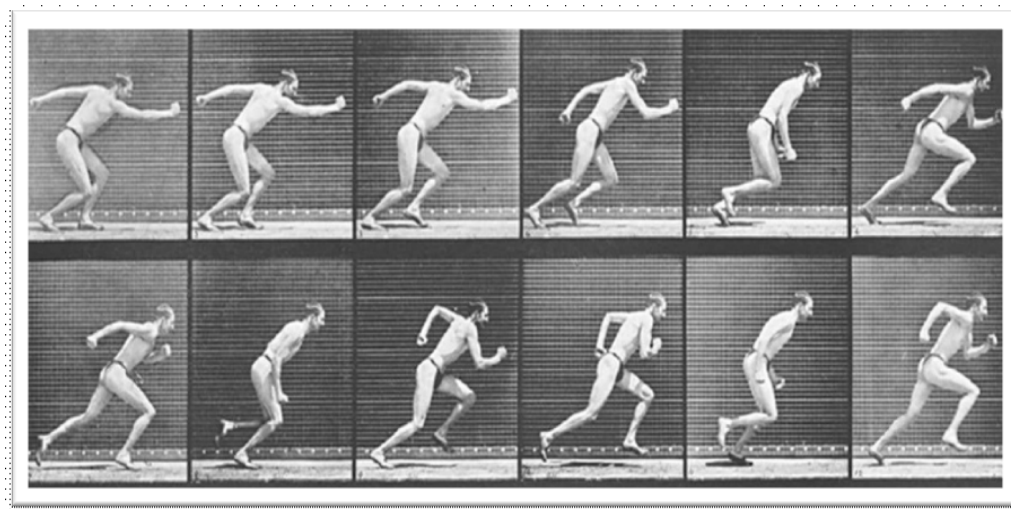


Figure 4 Man in motion (EJ Muybridge, Philadelphia, Photogravure Company of New York, 1887)

Muybridge certainly contributed to a revolution in the representation of movement in figurative art, with particularly at the Futurism (Figure 5, 6) and both Marey and Muybridge, due to the contribution, are considered as the founding fathers of the cinematography.



Figure 5 Umberto Boccioni: elasticity (1912) oil in canvas, 100 x 100 cm,
Civic Gallery of Modern Art, Junker Collection, Milan (Italy)



Figure 6 Giacomo Balla: Dynamism of a dog (1912) oil in canvas, 90.8 x 110.2 cm,
Albright Knox Art Gallery, Buffalo (New York City)

Wilhelm Braune (1831-1892) and Otto Fischer (1861-1917) were the first to describe the movement on three Cartesian planes, using their "Stereo-photo-grammametry" (Figure 7), direct measurements on images in time sequences. They were able to calculate trajectories, speed and acceleration of points of anatomical landmarks using fluorescent "markers" applied to the lower limbs [5].

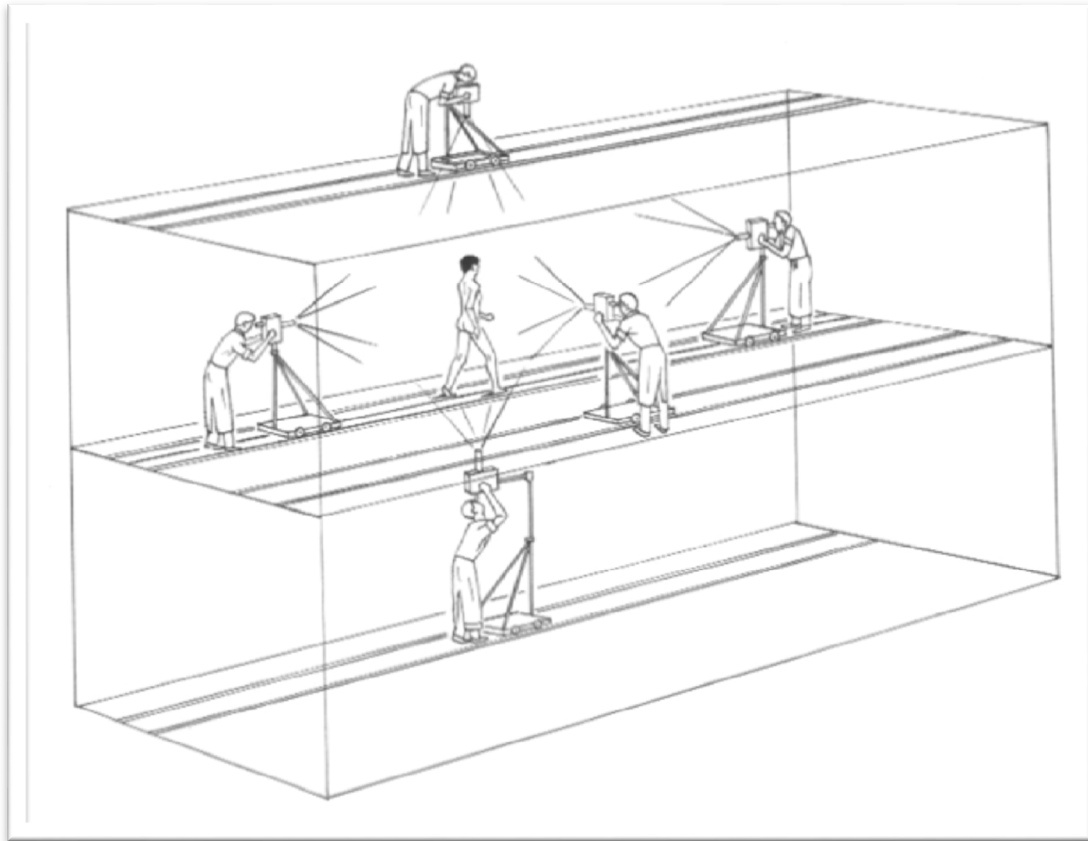


Figure 7 The first "multidimensional" shooting techniques of cinematography (Reprinted from Braune W, Braune W, and Fischer O. The human gait. Translated by Paul Maquet, Furlong R. Springer-Verlag, Berlino, 1987)

In first decades of the 19th century, Nikolai Bernstein at Moscow continued and expanded their studies improving resolution and frames frequency, with the possibility to observe new aspects of movement. In particular, he studied the relationship between the mass center and body segments during motion. His work became known all around the world only in the 60^s but still maintain its considerable originality, in particular the vision between mental programming and mechanical execution of movement [6].

The kinematic analysis progressed quickly with the development of high-speed photographic techniques. It worth mentioning the strobe technique, which consists into photograph the moving subject, "marked" by lines or clear points, in a dimly lit and with a dark background; the camera shutter remains open for long periods while the subject is illuminated by high frequency "flash" so that in the photo "markers" trajectory will stand out clearly from the background [7].

Also, in the first decades of the 20th century, the first electro-goniometric recordings of the joints range of motion make their appearance (Figure 8).



Figure 8 Electro goniometric recordings of joint's range of motion, during walking.

Source: Elftman H. The measurement of the external force in walking. Science 1938; 88:152-153

With the arrival of the first force-platform, designed by Herbert Elftman (1938, Figure 9), dynamics became finally accessible. This instrument permitted to measure the forces applied by the body to the surface. In 1940, thanks to the studies of Richard Scherb, the study of muscle contractions during walk through surface electromyography (EMG) became possible. Also, Verne T. Inman made a first systematic study of the normal human walk. The results were collected in his work "*Human Walking*", published in 1981, and still represents an all time classic [8].

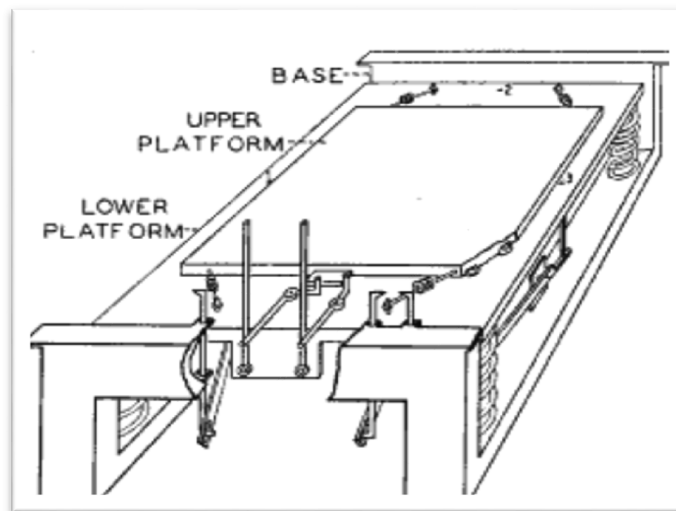


Figure 9 The first force platform designed by Herbert Elftman that permitted to measure the forces applied by the body to the surface. Source: Elftman H. The measurement of the external force in walking. Science 1938; 88:152-153

Motion analysis was expanded in the last decades with the study of previous unexplored aspects: the consumption of energy, studied by Rodolfo Margaria (1901-1983), and the "pendulum" mechanism of con-

servation of mechanical energy during motion, firstly studied qualitatively by John B. De CM Saunders and then quantitatively and systematically by Giovanni A. Cavagna; moments and joint powers were studied by David Winter and Antonio Pedotti. Systematic data in relation to age and sex were acquired enriching the established knowledge of human physiology. The development of electronics and information since the 70^s allowed the simultaneous acquisition and analysis of numerous variables, allowing experiments of relatively short duration and complex and accurate measurements in short time [9].

The major accessibility of technical and instrumental methods made also possible a systematic study of walking alterations in pathological motion patterns. The clinical and instrumental analysis of gait in patients with disabilities and specific rehabilitation techniques have become a key issue in the specialized training in Physical Medicine and Rehabilitation and the data collected become an integrate part of the future medicine.

THE MOTION

The gait cycle

Lower limbs movements are repeated cyclically. The time interval between the occurrence of a certain configuration of the spatial relationship body-environment and its repetition is defined as the step period (*stride period*). The semi-periods of the left and right limb (*step period*) under physiological conditions are identical. The events enclosed in the period are defined globally cycle. For clinical purposes cycle is divided into phases and each of them characterized by a particular event (for example, the ground-foot contact). Traditionally, step sequences begin with the right side (Figure 10) [11].



Figure 10 Foot position during gait.

In English *walk* and *gait* are used to indicate the motion. *Gait* should recall the more general concept of "mode of transport". Nevertheless, the scientific literature uses the two terms interchangeably. The distinction between locomotion and walking or gait, instead, remains clear. *Locomotion* is a more general

term that indicates the transfer into the space with autonomous production of work. For example, in biology it is applicable to swimming, fly, moving with a wheelchair or on skates, etc.

Characteristics of the gait: cadence, average speed and stride length

Cadence (step frequency) is the number of steps made in the unit of time, usually the minute (steps/minute). The inverse of the cadence defines the period of the step: duration of the step. While cadence is expressed in $\text{steps} \cdot \text{min}^{-1}$, period is usually expressed in seconds. The average speed of walking, V_{med} , is usually expressed in $\text{m} \cdot \text{s}^{-1}$ and is the result of the product of cadence and step length, expressed in meters. However it is still used to express V_{med} in $\text{Km} \cdot \text{h}^{-1}$.

Simple relations expressed from following dimensional equations relate the different measures:

$$\text{Period (s)} = (1 / \text{frequency}) \cdot 60$$

$$V_{\text{med}} (\text{m} / \text{s}) = (\text{rate} / 60) \cdot \text{stride length}$$

$$\text{Stride length (m)} = V_{\text{med}} \cdot \text{period}$$

$$V_{\text{med}} (\text{m} / \text{s}) = V_{\text{med}} (\text{km} / \text{h}) / 3.6$$

$$V_{\text{med}} (\text{km} / \text{h}) = V_{\text{med}} (\text{m} / \text{s}) \cdot 3.6$$

When we ask an adult healthy man to walk normally, choosing his speed and cadence, the follow parameters can be obtained:

$$V_{\text{med}} = 1.2 \text{ m} \cdot \text{s}^{-1} \text{ or } 4.32 \text{ Km} \cdot \text{h}^{-1}$$

$$\text{Cadence} = 110 \text{ steps} \cdot \text{min}^{-1}$$

$$\text{Stride length} = 65 \text{ cm}$$

Under these conditions the length of the stride corresponds to about 75% of the stature.

Phases and events of the normal human gait

During the gait cycles seven fundamental events, that are cyclically repeated, can be observed: the first four establish the *stance* phase and the last three the *swing* phase.

Any event may be chosen as the start of a particular phase and the gait cycle in general. Generally the instant in which the right foot comes into contact with the ground is used; in healthy adults this instant coincides with the heel-ground contact. The gait cycle ends when the right heel touches the ground again.

The left leg has the same events of the right step, half cycle shifted.

With reference to the right leg, we can identify:

1. Heel strike (initial contact with the ground)
2. Opposite toe off (detachment of the contra lateral toes, posterior)
3. Heel rise
4. Opposite initial contact (contact of the contra lateral foot)
5. Toe off
6. Feet adjacent (adjacent feet, medial malleoli on the same frontal plane)
7. Vertical tibia

In normal conditions, space and time aspects between two consecutive steps are quite similar. In case of diseases differences can be observed. For this reason it is useful to define the anterior and posterior step, spatial concepts and not temporal, referring to the phase of the double support to the ground. The posterior right step is defined by the distance between the right and left heel when the left heel touches the ground (heel strike). The distance between the left and right heel, when the right heel touches the ground, defines the anterior right step.

The stance and swing phases are the result of the cycle division using the time as a criterion. The swing phase starts when the foot is detached completely from the point of support (toe off).

Both beginning and the end of the support, include a period of bilateral contact or double support (*Double stance*) contrasting a period of the single stance that begins when the contra lateral foot is detached from the ground and then begins to swing. During the single stance phase the whole weight body goes to the single leg, as well as the forces, added or subtracted, due to the acceleration of the body upwards or downwards (during an intermediate walking speed the body weight decreases or increases of 10% approximately). During the single stance phase, all the forces that determine reactions from the ground in any direction are applied to the leg.

The duration of a single stance phase represents a very useful index in clinical practice to assess the ability to support the limb itself. Normally this time decreases when there are neurological or orthopedic problems involving the limb itself, which "calls for help" the contra lateral limb, so that early double support can be ensured. The double support begins with the ground contact of the other foot (contra lateral initial contact) and continues until the limb that it was in support initially stands out for the swing phase (ipsilateral toe-off). Each double support occupies about the 10% of the cycle and the major muscular work, necessary to move the body, occurs in this phase of the cycle (Figure 11). The temporal relationship between single and double support phases vary according to the speed of walking.

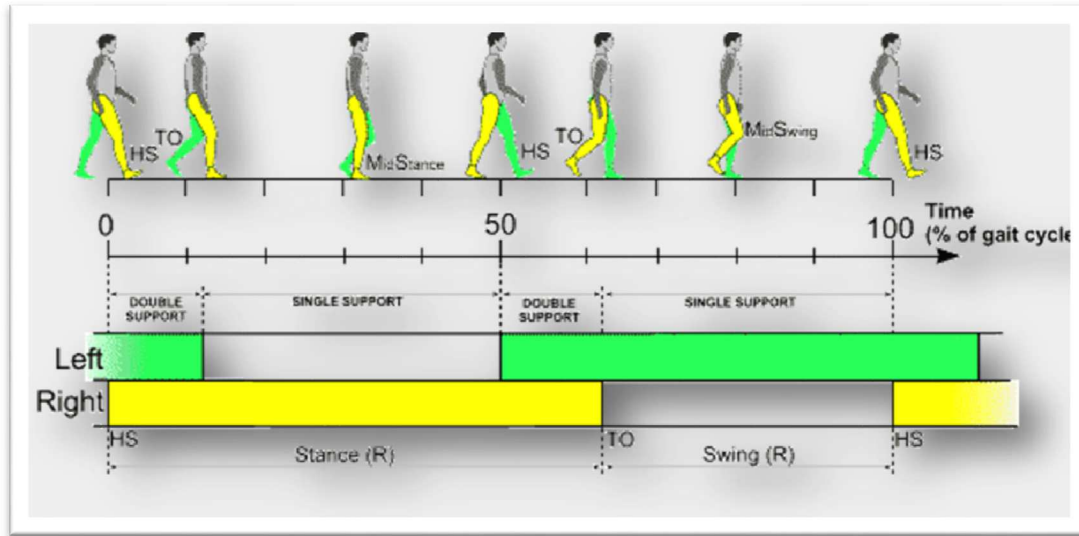


Figure 11 Single and double support during a gait cycle. The cycle conventionally starts with the initial contact of the right heel. Alternation of phases of support and oscillation for the two limbs and the corresponding periods of double and single support, expressed as a percentage of the gait cycle, are showed. Each double support phase corresponds to 10% of the whole cycle, while each single support to 40%. Source: <http://www.gla.ac.uk/t4/~fbls/files/fab/tutorial/anatomy/hfgait.html>

Limb's contact is conventionally divided into "load response", "intermediate support", "terminal stance", "pre-swing". The swing phase is instead divided into "initial swing", "mid swing", "terminal swing."

In 1992 Perry described the action of the foot and neck-foot during the stance phase dividing it into 3 "rockers", which correspond to the load response (loading-response- heel rocker), the mid-stance (ankle rocker) and terminal-stance (forefoot rocker) (Figure 12) [11].

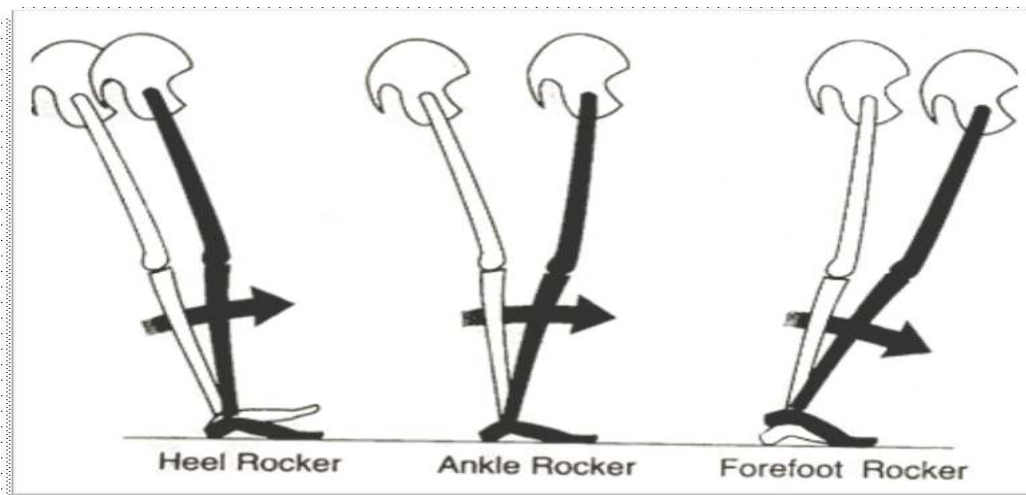


Figure 12 The three rockers described by Perry (heel, ankle and forefoot rocker).

Source: J. Perry, *Gait Analysis. Normal and pathological function*. Elsevier Italia, Milano, 2005

1. The first rocker begins with the initial contact of the heel with the ankle in neutral dorsiflexion and continues until to obtain a load -response; in the normal walk the fulcrum of this first rocker

is represented by the heel. As the ground reaction force passes through the heel, the immediate effect that is created is the complete support of the foot to the ground. The external moment (consisting in the GRF-Ground Reaction Force) is opposed by the internal moment (represented by the action of the pretibial muscles – anterior tibialis, extensor digitorum longus, extensor hallucis longus and peroneus third- that contract eccentrically during elongation causing deceleration); therefore, the first rocker muscle moment is a dorsiflexion moment.

2. The second rocker begins when the whole plant of the foot is in contact with the ground; an anterior displacement of the tibia is observed and the fulcrum is represented by the ankle joint. Since the GRF passes in front of the fulcrum, tends to bring the foot to further dorsiflexion. The eccentric contraction of plant flexor muscles (Soleus) is opposed and, therefore, the second rocker has a plantar flexor moment.
3. The third rocker begins when gastrocnemius and soleus are activated causing an acceleration force through the concentric contraction that blocks the progression of the tibia.

Schematically phases and events of the human gait cycle are represented in Figure 13.

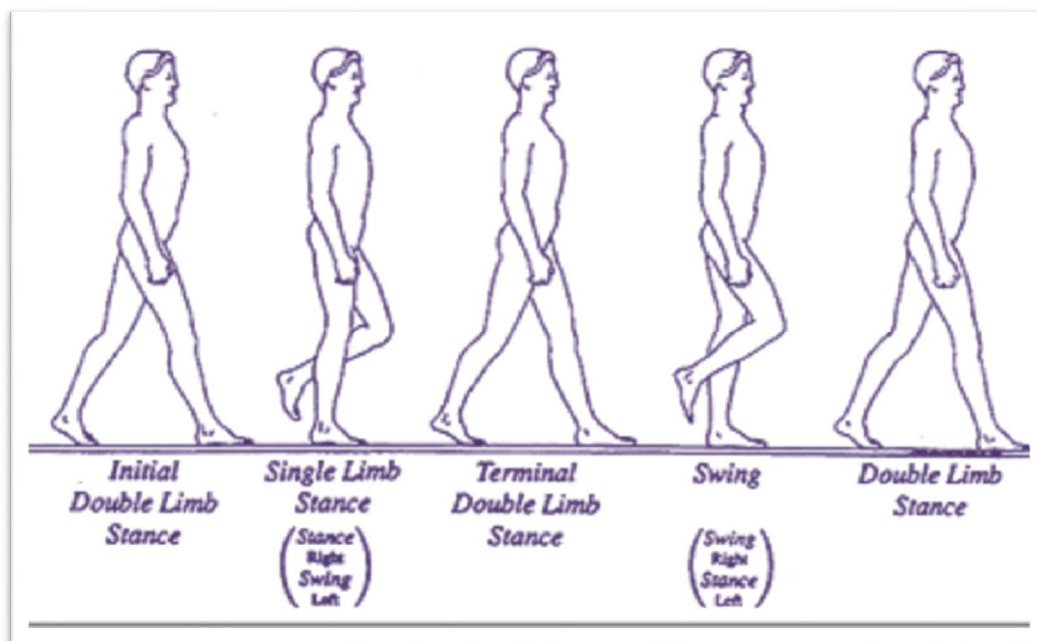


Figure 13 Phases and events of the human gait cycle.

1. Initial contact with the ground (**Heel strike**): contact between the heel and the ground. The ankle joint is in a neutral position, while the knee is extended and the hip flexed approximately of 30°.
2. Loading response: in this phase the foot touches completely the ground and the ankle has a slight plantar flexion (about 10°). The absorption of the impact is guaranteed by the quadriceps that resists at the knee flexion, making it gradual. Also, the "calcaneus rolling", decelerated by the muscles of the anterior compartment of the leg, contributes to the absorption of the impact and to

- body's progression. Movement at the hip is minimal to stabilize the trunk on the limb that accepts body weight. It is a very short phase, ranging from 0 to 10% of the entire gait cycle.
3. Detachment of the contra lateral foot: corresponds at the end of the double support phase. The right foot becomes flat, while the left foot begins its detachment from the ground supports body weight.
 4. Intermediate support: at the beginning the ankle is in neutral position and the foot is completely flat. In the second part, however, the body is located on the forefoot, but the heel is still in contact with the ground. The dorsal flexion movement of ankle permits the progression, and the progressive extension of the knee increases limb's stability in loading. The action of the abductor muscles stabilizes the pelvis horizontally, providing a good basis for alignment of the trunk. As the limb rotates forward on the foot, the critical point for the dynamic stability is moved from the knee to the ankle. This phase ranges from 10 to 30% of the gait cycle.
 5. Detachment of the heel: very variable phase that depends on the gait speed.
 6. Terminal support: In this phase the heel is further detaches from the ground. The rotation on the forefoot allows the body to advance beyond the supporting limb. The dynamic stabilization of the ankle joint is an essential element for the detachment of the heel. The limb, passed the vertical and the body, begins the "free front fall" that allows progression but, also, represents a source of instability. The result is a further ankle dorsal flexion with the knee slightly flexed, due to the body weight. This phase ranges from 30 to 50% of the gait cycle.
 7. Contact of the contra lateral foot: takes place during the swing phase of the right foot.
 8. Pre-swing: at this phase "pushing" actions occur that determine the oscillation of the limb and weight transfer is observed. Metatarsus-phalanx joints are in dorsal flexion, while the ankle is in plantar flexion. The knee is flexed and the hip is in neutral position. This phase ranges approximately from 50 to 60% of the gait cycle.
 9. Detachment of the toes (*Toe off*): total transfer of the body weight to the contra lateral limb, so the right limb can advance.
 10. Initial oscillation: the limb is relieved from the ground. The hip and the knee are flexed and the ankle's plantar flexion is reduced. Foot's detachment depends from knee flexion, since the set back position of the limb leads the foot in a position with the fingers facing down. The rapid forward rotation of the thigh determines an important propulsive force. This phase ranges approximately from 60 to 73% of the gait cycle.
 11. Adjacent feet: in this phase the limb in oscillation passes over the limb in support and the two feet are located next each other.
 12. Intermediate oscillation: increase of the hip flexion and reduction of the knee flexion. The tibia is in vertical position and the ankle in a neutral position. The active control of the ankle joint allows the foot to rise from the ground. The limb moves in relation to trunk from a posterior to an anterior position. Initially the ankle is flexed, due to the anterior tibialis action, and after regain the extension that had pushed the body in forward at end of the support phase. This phase ranges from 75 to 85% of the gait cycle.

13. Tibia in vertical position: in this phase the limb in oscillation is located with the tibia in a vertical position.
14. Terminal oscillation: is a transition phase between oscillation and support. Progressive movement of the limb continues with the extension of the knee. The ankle remains in its neutral position to place the foot in an optimal position when the initial contact with the ground begins.

Sequence of the muscle activity during gait

During gait muscles activation occurs according to a sequence tightly related to the phases and the speed of gait (Figure 14). The majority of gait does not require the participation of muscles and almost the whole oscillation phase is due to gravity and inertia [7,12,13].

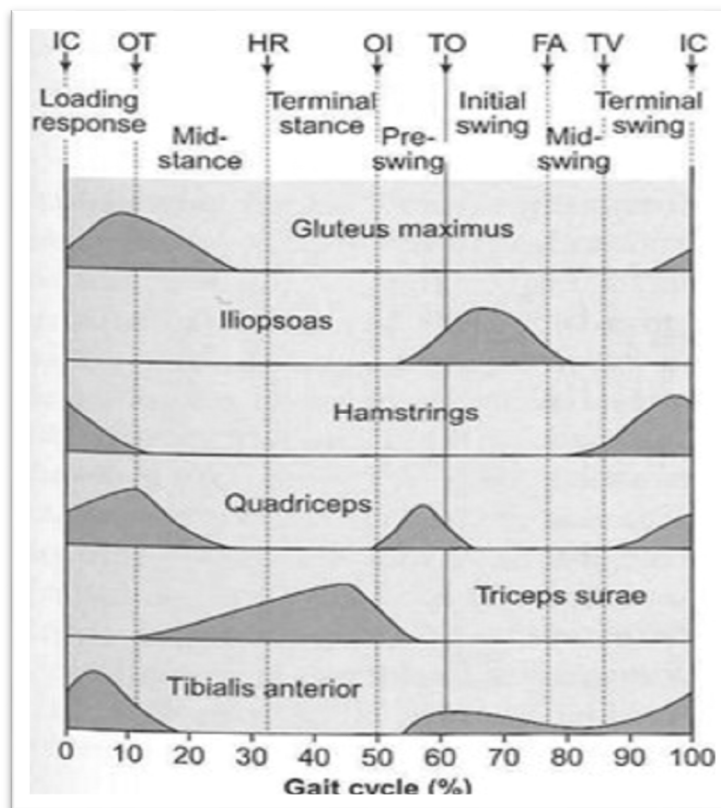


Figure 14 Muscles activity during gait. X-axis shows the time (% of gait cycle) while the ordinate muscles activity (mV) during gait. IC: initial contact; OT: opposite toe off; HR: heel rise; OI: opposite initial contact; TO: toe off; FA: feet adjacent; TV: tibia vertical.

Source: Whittle M.W. Gait analysis: an introduction. 4 Edition. Butterworth Heinemann Elsevier, Oxford, 2007

During the heel contact (phase of load acceptance) we contract:

- the dorsal flexors muscles of the foot: to stop the fall of the tip of the foot;
- the quadriceps: amortizing action;

- the hamstrings: to facilitate the hip to pass from flexion to extension, allowing the passage of the body weight to the foot, even through the quadriceps fixation.

During the full support we contract:

- the plantar flexor muscles: decelerate the forward fall of the body and start the push of the foot;
- the gluteus, tensor of fascia lata and erector muscle of the rachis: stabilizers of the pelvis during the single stance phase;
- the intrinsic muscles of the plant of the foot: stabilize the different foot joints during the push off phase, acting mainly at the subtalar and midtarsal joints.

At the toe off phase we contract:

- the quadriceps: to limit knee flexion due to gravity;
- the hamstrings: opposition to the hip flexion caused by the trunk;
- the adductor muscles: opposition to an excessive shift of the pelvis to the side of limb support.

During the swing phase the anterior tibialis and the others dorsal flexors have a moment of relaxation, which coincides with the maximum plantar flexion of the foot. In this phase the contracted muscles are:

- ilio-psoas and sartorius: accentuate the fall in flexion of the thigh;
- biceps and gracilis: to lift the flexed leg to the knee;
- hamstrings and gluteus maximus. Decelerate the oscillation of the limb and absorb part of the impact with the ground (at the end of the swing), while the dorsal flexors muscles control the position of the foot;
- hamstrings: stop the flexion of the thigh and then the extension of the leg (double control, according to their lever arm).

The contraction of the erector spinae at the beginning and at the end of the stance phase prevents the forward fall of the trunk caused by the rapid deceleration of the pelvis at the time of the heel strike.

Regarding the upper limbs a pendulum movement is observed during gait without any deltoid activity, and stops when the antagonists become active.

Specificity of the gait in childhood

Humans walk reaches maturity only around the 7th year of age as a result of the maturation and integration of the sensory, motor and the bony-muscle systems.

Environmental influences have considerable importance in the acquisition of the walk, as well as the psychological and somatic maturation: children who have little or poor human contact, in terms of culture and emotions, may present a delay on acquisition of the walk or in some cases do not acquire the bipedal walking.

In newborns, movements that are similar to children's walk can be observed. Supporting and pushing forward, but slowly, the newborn's feet in contact with a surface of support, we can observe reminiscent movements of the morphology and sequence of the walk (reflex of the automatic walk, Figure 15) [14]. However, these are reflex movements that disappear within the first two months of life and represent a sign of central nervous system immaturity. In this age, ability of autonomous support, balance maintenance and a precise direction of the walk are missing.

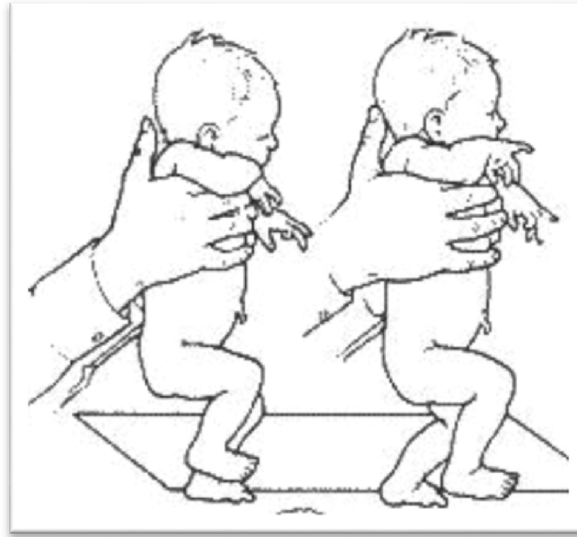


Figure 15 Invocation of the automatic reflex of walk.

Source: Baldissera F, Bartoli E et al. *Fisiologia e biofisica medica*. 2nd Edition, Poletto Editore, Milano, 2002

The physiological age for the beginning of the walk is around the end of the first year of life, shortly after the acquisition of upright posture. At this early stage, the mechanical and nervous characteristics (defined as "pattern") present characteristics of immaturity (Figure 16) [15]:

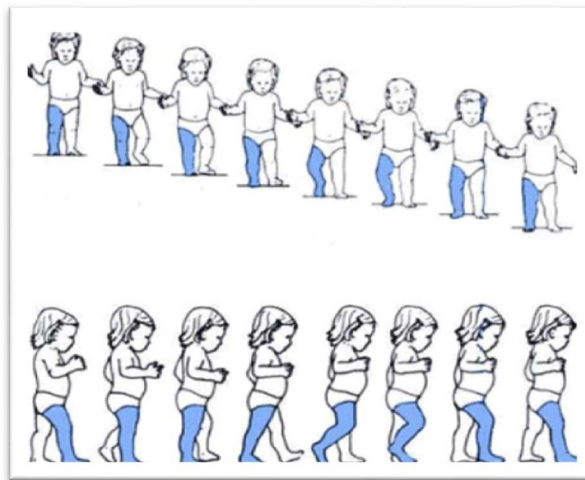


Figure 16 Normal gait cycle at the first year of life, in frontal and lateral view. Source: Fedrizzi E. *I disordini dello sviluppo motorio. Fisiopatologia, valutazione diagnostica, quadri clinici, riabilitazione*. Piccin Edition, Milano 2004

- the co-activation of flexors and extensors muscles (newborn's "Stepping") persists and determines simultaneous movements in all joints. Electromyography shows a tendency to recruit the majority of the muscles for a higher proportion of the gait cycle;
- wide base support;
- the initial contact begins with the entire plant of the foot and does not with the heel. In fact, the contraction of the tibialis anterior muscle in the final phase of the oscillation (swing), typical of the mature walk, is replaced by the contraction of the triceps that determines a support on the plant or on the toes. The ankle is in plantar flexion at the time of the contact to the ground and remains in the same position during the initial phase of support (stance);
- in swing, the whole lower limb remains externally rotated and during the stance, knee flexion is minimal or absent;
- the pendulum movements of the upper limbs are absent and replaced by a fixed position in flexion and abduction that probably aims to facilitate balance;
- the trunk takes on a pendulum motion in the frontal plane (front pendulum);
- the whole gait cycle is shorter than in adult (approximately 0.83 sec in 3-4 years children, while 1 sec in an adult). Cadence is increased while speed and stride are decreased (around 1m in children aged 3-4 y).

Symmetry of the space-temporal parameters of the step between the two sides is evident since the early first steps and remains in all ages. The swing phase occupies a smaller part of the gait cycle in children compared to adults. The relative duration of the swing phase increases during the first years of life, and reaches duration like in adults around the age of four (Figure 17) [15].

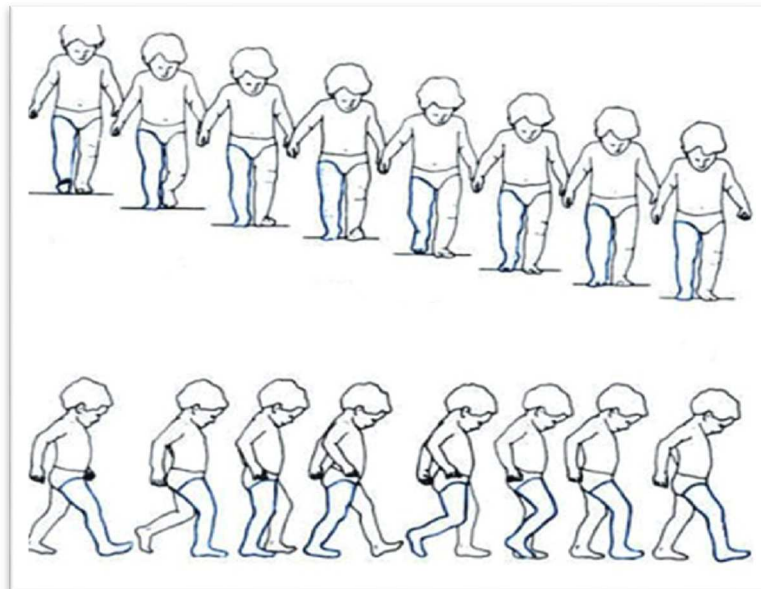


Figure 17 Gait cycle in 2-years child. Knee flexion in the stance phase and initial contact to the ground by the heel are noticed.
Source: Fedrizzi E. I disordini dello sviluppo motorio. Fisiopatologia, valutazione diagnostica, quadri clinici, riabilitazione.
Piccin Edition, Milano 2004

The autonomous walk is indicative of the maturation of the brainstem and of the reticulo-spinal pathways and is the result of maturation of the vestibular and cerebellar systems for the control of the posture.

The walking pattern begins and takes the first features of adulthood at the end of the second year of life (Figure 17): the base of support is reduced thanks to the decrease of external rotation - abduction of the hip. The upper limbs are abducted and extended, allowing the appearance of first alternate movements of the arms. These movements are subject to progressive changes up to four years. In addition, foot's dorsal flexion before heel strike becomes more evident.

Maturation of the walk is reached around the age of 7 years, when the pattern becomes similar to that of the adult. At this age the child has acquired the voluntary control of speed and cadence as well as the ability to change movements in relation to the different characteristics of the ground.

The length of the stride increases gradually until the growth ends, with a peak speed of growth around the age of 4 years. Around 7 years reaches 114 cm and the stride length is about 0.85 sec [15].

METHODS TO STUDY THE MOVEMENT

The general principles and methods of the study of the different aspects of movement vary according to the level of observation. The segments and joints that move in space represent the global level of the movement. The study of this level is based on principles of kinematics so such as they are described in classic physics: practically we have to identify the position and the speed of the segments or joints to analyze. This level can be also studied through the simple visual observation, which offers only a generic qualitative assessment of the trajectory or the direction of movement and a very rough estimation of its speed. For a proper analysis, kinematics specific methods and equipments are required.

The study of the kinematics, therefore, provides a description of the movement in space and time, but does not provide information about the causes that induce the observed displacements. The following level of study is represented by the analysis of a muscle in generating forces capable to rotate joints and move bony segments. For this reason, to understand the mechanisms that produce the movement of the joints or stabilize them during the maintenance of posture, it is important to study the dynamic of movement.

The study of the biomechanics of movement can therefore provide precise quantitative details and can describe the motor behavior observable from the outside.

Although the biomechanical approach also allows to represent the nervous processes on motion control, the study of activation of muscles by electromyography provides a deeper insight to study the actual generation mechanisms of gait. Electromyographic analysis of a set of muscles during a single muscle action can capture important information regarding the organization of muscle synergies, at the base of motor coordination.

Kinematics

Kinematics describes spatial-temporal aspects of the movement, without reference to the forces. Analyze the kinematics of a movement means, therefore, to identify the position and speed that in each instant characterizes the displacement, linear or angular, of every part of the body in motion.

The instruments, that can record the position of a body in motion, capture the coordinates with a specific frequency of sampling. The sampling frequency is measured in Hertz (Hz), and is determined by counting the number of coordinates recorded every second. Each instrument may present different values of its sampling frequency, but during the detection of a movement the sampling frequency remains constant, and then remains unchanged even though the interval between the various points of the trajectory.

The equipment able to provide information on kinematics is based on systems capable to detect the Cartesian coordinates of parts of the body or the angular variations of the joints. A common technique is based on instruments that detect signals from a set of markers applied in correspondence of the body part that is to be analyzed. According to the used equipment, the markers can be passive or active. In the first case they are illuminated by a proper light source and reflect optical signals to a camera, while in the second case they are devices that actually produce and transmit signals (for example, ultrasonic signals or light signals). The use of passive markers presents the benefit of make the subject free from wires connected to markers. In the other case, instead, the markers must be powered so they are connected to wires that can reduce the range of studied movements. The components that receive signals from the markers (cameras, acoustic devices or optical) are connected to a computer and they can transform the signal in the spatial coordinates of each individual marker.

Alternative techniques are electro-goniometers and accelerometers. The electro-goniometers are applied at the joints and measure the angular variations of individual joints. The measurement of the position, therefore, will be expressed in terms of angular degrees and the speed will be expressed in degrees per second. The accelerometers, however, measure the acceleration of points or segments of the body and not the position of the body or of its parts.

Optical Systems

An optical system for motion capture is constituted by a set of cameras that surround the scene where the subject is moving. The movement is measured processing the images captured by the cameras. Recognizable markers applied on body landmarks can be used, or their position can be "marked" and identified on the video in subsequent images. The systems currently on the market allow automatic "tracking", while up to thirty years ago it was necessary to calculate the articular angles of any single frame. The advent of optoelectronic systems made this method obsolete. If a simple shooting digital video is needed, however, there are now systems that automatically recognize landmarks that an operator should identify on the video image. The systems perform an automatic "tracking", as long as the referent target appears on the video image with sufficient contrast respect to its background.

Stroboscopy is maybe the more ancient modality of optical detection of markers, as already mentioned in the introduction. Substantially stroboscopy is a form of high frequency lighting. The subject is "immortalized" in each single frame as if it was stationary. The technique is now obsolete, since turning on and off the incandescence lamps required around 50 ms, corresponding to the sampling frequencies of the markers of 20-40 Hz (Figure 18).

Nowadays, light sources emitting diode (LED) are available, and they allow higher frequencies (hundreds of Hz). The used emission is typically in the infrared spectrum and the registration is no longer based on the chemical principles of photography, but on digital videos. The idea of a "digitization" of the record of motor marker, however, is certainly today known due to the pioneers of the strobe.



Figure 18 The strobe lightning is the base of the most famous contemporary dance: Caught ballet, that was created by David Parson in 1982. It is easy to imagine how a number of light spots centered at the right time on the dancer against a dark back round, can give the illusion of seeing extraordinary fly of the dancer Source:https://www.behindtheshutter.com/wp-content/uploads/2014/11/MCorentino_BlogLarge_Nov14.jpg

Optoelectronic optic systems

The optoelectronic systems represent the gold standard for kinematic analyses. As already written, two basic techniques are used: video with passive or active markers applied to the skin at anatomical bony landmarks. In the first case they merely reflect light, usually emitted by a source surrounding the same camera that record the reflections. The cameras, suitably spread in the environment, are connected to a computer that can transform the signals captured from multiple cameras in the spatial coordinates, through trigonometric calculations and a previous calibration (Figure 19).

The sampling frequency could be very high (commercially available systems are capable to sample from 120 to 3000 Hz). The spatial resolving power is very high: in a volume of about 15 m³ is in the order of fraction of a millimeter.

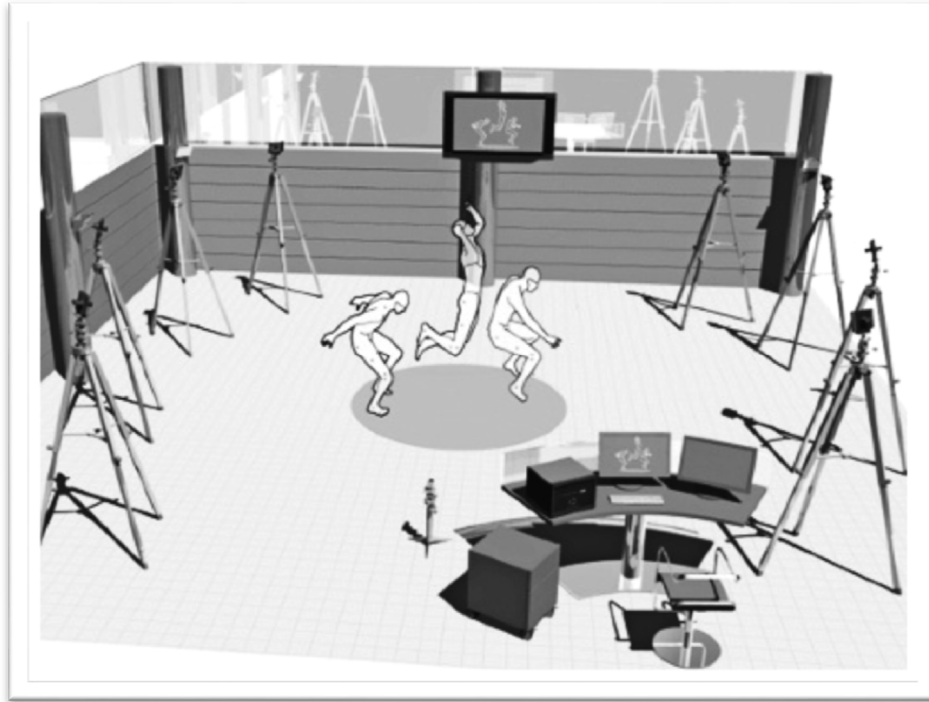


Figure 19 Image of an optoelectronic system. Source: <http://www.analisedelmovimento.it>

Kinetics

The joint moments are responsible for the physical condition of static or dynamic motor control. The forces that produce the angular rotation of the joint determine displacement of each segment. Each joint is subjected to 'the action of various forces' generated in part by the muscles and in part due to the loads and to the resistance applied on the body segments. The ability to move or maintain a stable articulation, then, depends on the interaction between the forces acting on the body.

The muscles represent the active component of the loco motor system and they are under continuous monitoring by the nervous system. The ability of the nervous system in determining the muscular forces, useful to the motor control, depends on the possibility of representing the whole biomechanical system, including passive components such as bone structures, ligaments, and loads that act on it. In particular, it is necessary to evaluate the muscle forces on the basis of the effects these will have on the rotation of the joints. The more correct way to figure out the mechanisms of production of strength during posture or motion is to outline the bony segments as lever arm systems [16].

The elements of a lever arm are represented in figure 20. The nervous central system determines the muscle strength on the basis of the moments of muscle strength and moments of resistance. The moment of a force is the physical element, which allows evaluation on the effect of the force on a segment that is free to rotate around a fulcrum.

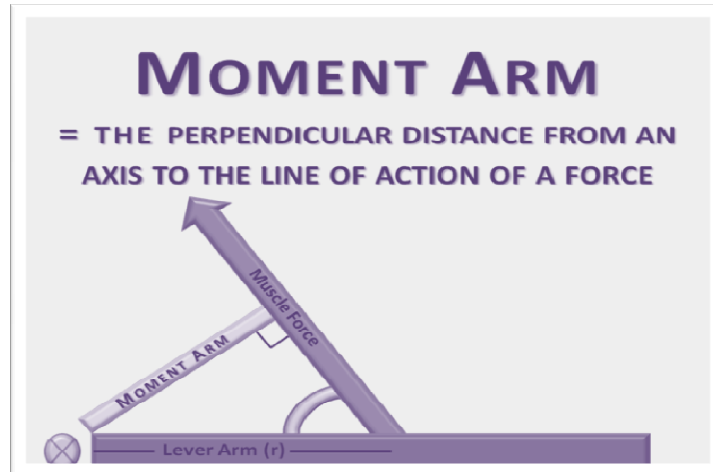


Figure 20 Elements for the study of the lever arm

The importance of the force moments to determine the value of the voltage that the muscles need to develop and produce movements or posture is clear. If one wonders what should be the muscle tension that the biceps must develop to counter a force load of 5 kg, which would tend to extend the forearm, you might think incorrectly that it would take a force equal and contrary. This setting it would be correct in case of strength applied to bodies moving in straight lines, but the bony levers are bodies that revolve around the articular fulcrums and so the force moments should be considered.

Regarding the example, considering a force of 5 kg weight applied 30 cm from the fulcrum that produces a moment of $150 \text{ Kg} \cdot \text{cm}$, the biceps brachial muscle, situated 5 cm from the fulcrum, must exert a force of 30 kg to produce a moment equivalent to that of the load, thus allowing the maintenance of static equilibrium of the elbow. If, however, you wish to obtain the movement of the forearm on the arm, the value of the force produced by the biceps muscle must be such as to produce a higher moment (flexion) or lower (extension) respect to the moment of load. The flexed posture will therefore be guaranteed by a muscle strength far superior to that exerted by the load.

As it is well known from physics, this type of lever is not advantageous for the muscle strength (Figure 21). In other cases, muscular strength can be lower than the load necessary to produce an angular moment adequate to ensure balance. In fact, the case of the lifting movement of the feet is an example of advantageous lever (Figure 21): the fulcrum is placed in the contact point of the metatarsus with the ground; the weight of the body is the loading forces that discharge between the fulcrum and the force is produced by the triceps surae muscle. The arm of the force will be greater than the arm of the load and therefore the lever requires less muscle strength. The third example of a lever (Figure 21) presents an intermediate situation, where both arms can alternately be the largest, producing more or less advantageous situations.

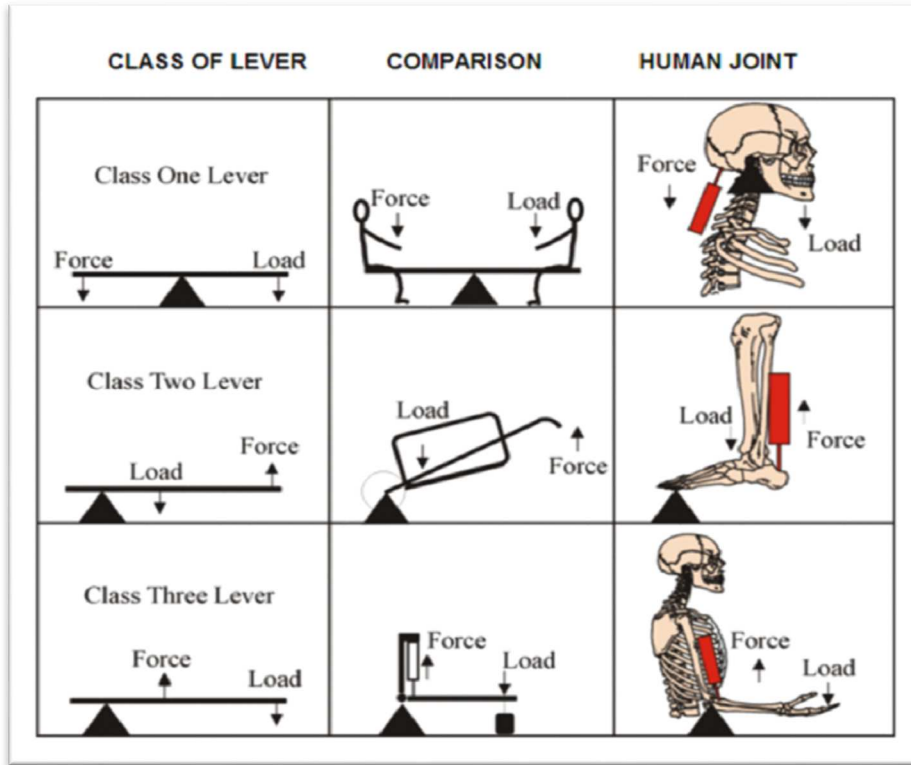


Figure 21 Examples of a type I, II and III levers. Source: <http://waergo.com/JES/BodyBasics.htm>

Although the simple principles based on balance of force moments are fundamental to understand the biomechanics of movement and posture, the complexity of the bony structures, joint and muscles of the loco motor system force us to consider a number of other important factors for the mechanical equilibrium of the joints. It is important to place emphasis on at least two of these factors: variations of the lever arm of the forces during the rotation of the joint, and the possibility to combine different muscular forces on the same joint.

For a correct measurement of the lever arm of the forces we must consider the straight line passing through the fulcrum and perpendicular to the axis of the force vector (the longitudinal axis of the muscle). The arm of the force is determined on this straight line by measuring the distance between the fulcrum and the point of incidence of the straight line on the force vector. As illustrated in figure 22, when the articular angle is modified, the distance between the fulcrum and the muscle axis can change by making variable the value of the moment of force of the muscle during the movement of the segments. Regarding the example of figure 22, during the flexion of the forearm on arm, the lever arm muscle strength increases and, therefore, with the same loading force, lower muscle strength will be required to maintain the articular balance or to generate motion.

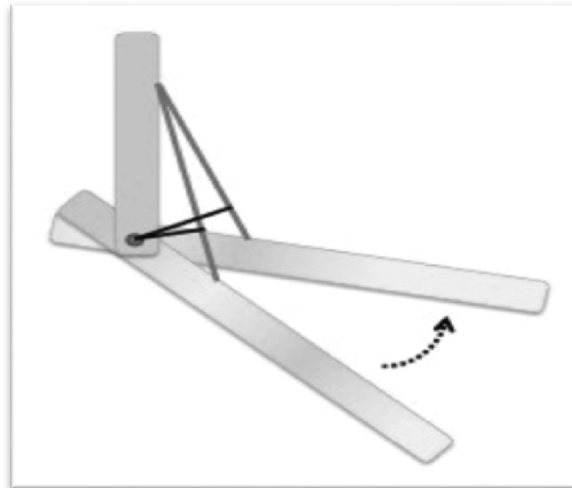


Figure 22 Schematic illustration of the variation of the biceps brachii lever arm length during the flexion of the forearm to the arm

Another particularly important factor to consider when you have to study the dynamic or static motion is represented by the multiplicity of muscles and related moments acting on a single joint. The case shown in Figure 23 shows two muscles, a flexor and an extensor, to control the elbow joint. Angular moment generated by the power load must be balanced by the combination of the moments produced by the two muscles. Since the two muscles act in opposite directions, the moment of muscle strength will be the algebraic sum of the moment of the flexor and the moment of the extensor. Following the arithmetic signs in Figure 23, when the moment between the two muscles will be equal to the time of loading, the joint will be stable; if, instead, the moment of the forces will be greater than the load, the joint would fall if the moment of the flexor prevails or go towards extension if that of the extensor prevails.

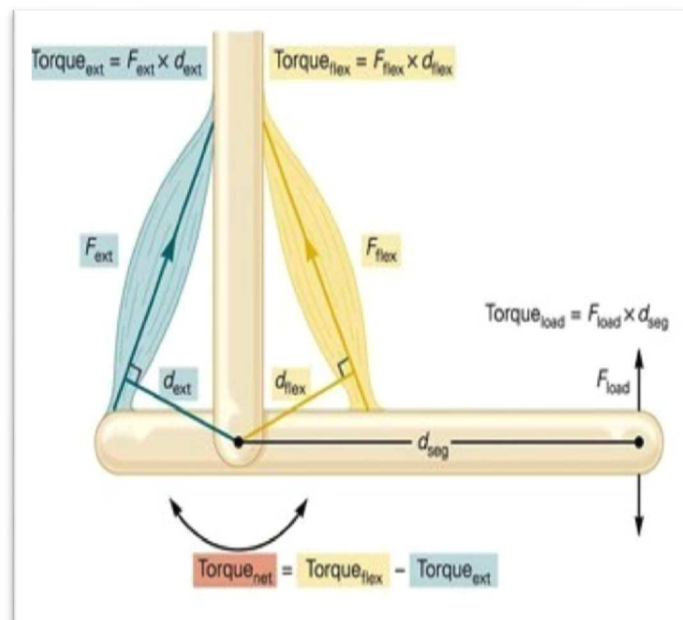


Figure 23 Diagram representing the combination of the moments (Torque) of two antagonistic muscles. To ensure the static equilibrium of joint, the net time (Torque net), resulting from the combination of the two moments, must be equivalent to the time of load (Torque load)

According to the previous considerations, it is clear that the system is actually very difficult to study when you consider the real number of factors that may affect the mechanics of joint movement.

In summary it can be said that the muscular strength, which depends on extrinsic (nervous regulation) and intrinsic factors (mechanical and morphological characteristics of the muscle), must counteract a series of natural resistance (tendons and connective structures of the joints) that, even in absence of external load, must be considered to assess the mechanical equilibrium.

A simpler way to facilitate the determination of the net moment applied to a date articulation is represented by the method of *inverse dynamics*. This method is based on the finding that the application of a set of force moments on joints produces an acceleration of the segment that rotates. In other words, the acceleration that undergoes the rotating joint is proportional to the net applied moment: if the moment increases, the angular acceleration will increase and vice versa. Based on these considerations, by measuring the acceleration of a segment that rotates around a joint, one can obtain an estimation of the net moment applied at that joint. In particular, the net moment of rotation around a joint can be obtained from the product of acceleration (a) for the moment of inertia (I): Net moment = $a \times I$. The moment of inertia is given from the product of mass (m) of the rotated segment multiplied by the square of the distance from its center of gravity of the axis of rotation (r): Acceleration can be measured using the kinematic methods described above and the measurements of the mass and the distance from the gravity center of the rotation axis are obtained by means of specific anthropometric tables.

This simple method of determination of the net moment is known as "inverse dynamics" because the measurements can be reversed due to the physical relationships between dynamic and kinematic: knowing the dynamics (forces and moments) you can learn about the body movements (Kinematic), and kinematics (Acceleration) can be determined by the dynamics (forces and moments).

Surface Electromyography

Muscular electrical activity can be obtained by electromyography (EMG). EMG signals originate from the electrical activity of individual muscle cells that are innervated by single motor neurons form the motor units.

Each motor unit, then, is made up from a single motor neuron and from fiber cells innervated by it. The activity of a single motor unit is derived from the sum of the action potentials of individual muscle cells that form the different units.

Even though each single potential of action of fiber cells is generated in the same instant and with same amplitude, the different distance that separates fiber cell from the recording electrode leads to a reduction and a phase shift of the original signal. In this way, the electrical signal that will be recorded by the electrode, called *potential of the motor unit*, can have different shape and amplitude.

The most common EMG techniques provide that the position of the electrodes remains fixed, so we can say that the amplitude of each single motor unit will remain constant for the whole duration of the recording.

Muscular activity is rarely limited at the activation of a single unit motor. The most common functional conditions involve the progressive activation of a certain number of motor units producing more complex EMG tracings. Indeed, in this case, the individual potential of the motor units are overlapped, interfering with each other.

The potential of each unit are clearly different and have the same amplitude when recorded separately. The shape of EMG will be, however, more complex when the recording will affect the simultaneous activity of more motor units. The overall activity of the muscle, therefore, produce unit signals that will interfere with each other more and more at the increase of muscle activation and the track will be identified as *interference EMG*.

Unlike the unit EMG, which requires the use of needle electrodes, the overall electrical activity of the muscle can be derived using metal electrodes placed on the skin surface. Through surface electromyography is possible to study the overall activity of individual muscles and synergies between different muscles during motor actions.

The overall activity of the muscle is recorded better through surface electrodes as they can have a wide-ranging collection. The interference activity is useful when exist the need to compare the methods of activation of different muscles during a motor act (muscle synergies).

The study of human movement: an overview

Important aspects of the movement can also be analyzed using individual approaches, but a full description of the movement can be obtained only when all the previously described methods are used.

The description of the movement in terms of kinematic, static, dynamic and electromyography, allows obtaining important information about the cause and effect relationships that exist between the different elements (biomechanical and electrophysiological) of the motor action.

The ability to master these tools for quantitative analysis of the movement is definitely a critical step for the knowledge of the causes that produce the motor performance and for the study of the movement in the fields of education, sport as well as in the areas of prevention and rehabilitation.

Study of treadmill gait

Commonly, gait study is performed on the ground through the use of platforms equipped with force sensors. Gait analysis performed on a treadmill with force sensors is very recent and less common.

The various models of platforms differ in the sensitivity and in the number of components of the force that can detect. Some models can detect only the vertical component of the force and some others can provide the three components of the applied force (vertical, lateral, antero-posterior), the torque moments

of force in the three planes and the two spatial coordinates of the center of pressure. The center of pressure represents the point on ground in which the resultant of force is applied.

The treadmill presents different practical benefits. Firstly, it allows walking under examination at a constant speed set by the operator. This permit us to repeat the test, for example, after the rehabilitation treatment, reproducing the same speed set. On rigid platforms subject's gait speed cannot be imposed from the outside and it is difficult to ask to the subject to walk at the same speed in subsequent tests.

Furthermore, the use of the treadmill allows the execution of numerous consecutive steps in a short period of time (typically 40-100 steps in a minute). Through the recording of more consecutive steps the subject is observed during a prolonged period of walk respect to what happens when fixed platforms are used. For example, it is possible to study patients with pain or risk of falling, who can perform repeated trials that cannot be obtained when using fixed platforms where you can record only a few steps for each gait and not always at the desired speed.

The analysis on treadmill allows reducing the time for the experiment. In fact we can get in a single acquisition a series of complete gait cycles, modulating real-time parameters such as the speed, and obtaining kinematic data of single and double support for one or both limbs.

An important disadvantage of the treadmill is that it cannot be used in patients using aids, or those who are unable to walk alone. Other disadvantages are related to possible fluctuations in the speed of the carpet. The tape can slip relative to the rollers. In fact, the engine, if not sufficiently powerful, can present a periodic deceleration due to the "fall in forward" of the body (treadmill and subject share a common dependence on acceleration compared to the surrounding environment). The treadmill is a much less rigid than a concrete floor, so the transmission of strength to sensors can result somewhat distorted. In addition, motors transmit mechanical vibrations and electromagnetic noise that are a source of noise in the signal's strength. Finally, there are biological differences between modest but secure gait on the ground and on the carpet.

The determination of the pressure center (PC) is maybe the more critic point. In practice the position is estimated from the distribution of the vertical forces between three or more sensors: as close as is the PC to a sensor, the greater the total fraction of force registered by that particular sensor. Asymmetries in the response of the sensors to the signal or noise can then bring to altered results.

The biological differences between walk on ground and on a treadmill are due to the fact that the individual tends to adapt slowly to the new situation, initially with an excessive frequency of steps (and therefore a length). In practice, the adaptation can be complete within a couple of minutes, with the tendency to use a shorter step and a higher cadence (about 8%) on a treadmill compared to what occurs spontaneously on the ground. Probably this difference is related to a sensory conflict: on the treadmill we "feel" to walk but it "see" our body firm and that causes more frequent short steps, during which the swing phase and the acceleration-deceleration of the body are lower.

According to the neurophysiologic and biomechanical considerations, the increase of the cadence does not substantially modify gait for the purposes of its clinical analysis.

THE FOOT

The foot is the organ responsible for the upright stance, gait and running and it is an extremely complex structure and in terms of anatomy and function.

Humans, in their ontogenetic evolution, become a living being with the major instability due to rising center of gravity and the narrowing of the area of support. Simultaneously, the foot has become an antigravity organ, as it uses the gravity force for the maintenance of standing and walking.

The morphogenesis of the foot

The foot, together with lower limb, originates from the sketch of the longitudinal ridges (ridges of Wolff) from the 27th day of the embryonic period and can be identified as the third segment of the sketch of the lower limb (in the context of which it is already possible to distinguish tarsus and metatarsus) already after the 42 - 43 day; on the 45 day furrows between the toes appear and on the 52 - 53 day the differentiation of the toes is already completed (Figure 24) [17]. Ossification of the lower limb is made using the endochondral model; it begins on the VIII week and continues every week proceeding from the distal femur, tibia and fibula, and the tarsal, metatarsal and phalanges.

Initially, the longitudinal axis of the lower limb is perpendicular to the longitudinal axis of the body and the pre-axial (tibial) and post-axial (peroneal) edges are respectively cranial and caudal.

Similarly the rounded sketch of the foot is first placed on the sagittal plane, parallel to the sagittal plane of the embryo, so that the future plantar surface watches medially. Around the end of the VII week of gestation internal rotation of the limb begins, which continues in the fetal period bringing the knee and the foot in the front position, for which the pre-axial edge become medial and the post-axial lateral.

From the embryonic to the fetal stage, the foot undergoes other morphological and positional changes. Starting from its equine position (180° respect to the leg), the foot changes its orientation in space during the differential growth of the leg bones.

Between the VI and VII week, the accelerated growth of the end of the fibula on the calcaneus and talus practices a force in supination, so that the lateral portion of the foot undergoes an increased growth for which the foot assumes the equine-varus-supinated position ("embryonic foot"). Subsequently, between the VII-IX weeks, the tibial growth practices a pronation push to the talus and calcaneus, so the consecutive growth of the medial portion of the foot, with an abductor push leads the forefoot to a neutral position and the foot in pronation ("fetal foot"); this phase ends at the XII week with the acquisition of the talo-valgus position.

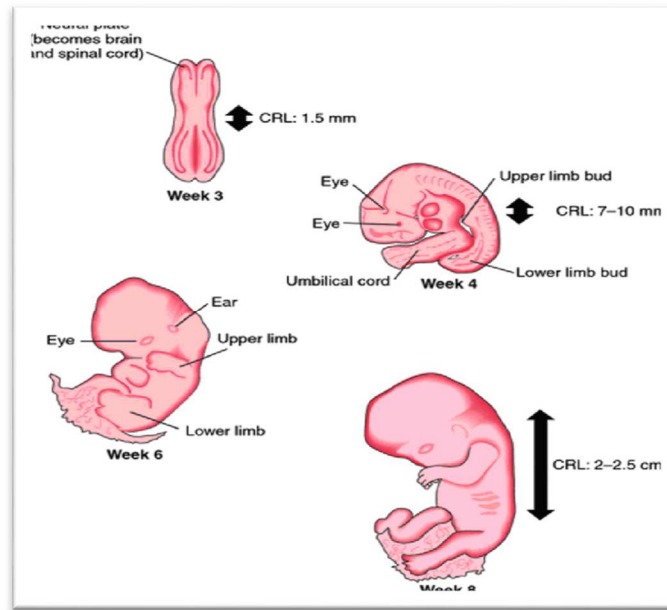


Figure 24 Morphogenesis of the foot. Embryonic development from three weeks through the eighth week after fertilization. Source: Pisani G. Trattato di chirurgia del piede. III edizione. Edizioni Minerva Medica, 2004

After birth, the valgus hind foot will tend to be corrected thanks to the peroneal growth and the intrinsic modifications of the tarsal bones reaching their final dimension around the age of 6-7 years.

Particular important are the changes that occur between the individual tarsal bones, and between them and the proximal epiphysis of the tibia; in the embryo, the tibia tarsal spacing appears in the distal-medial sense; gradually, this obliquity decreases and vanishes becoming horizontal towards the 8-10 years.

Initially the calcaneus (equine and with a very long anterior process) is lateral to talus, which has a neck-head portion larger than the body and directed downward and medially; the navicular bone is placed dorso-medially to the anterior segment of the talus. Subsequently (later in skeletal maturation), the body of the talus prones while the neck, reducing its size, becomes prone. Supination of the body of the talus determines subtalar migration of the calcaneus; the navicular bone goes in pronation and becomes congruent with the talus.

Anatomy and biomechanics of the foot and ankle

The foot articulates with the bones of the leg by the ankle, or tibio-tarsal joint; it is a trochlea and has, therefore, only one degree of freedom, conditioning the movements of the leg on the sagittal plan. It also has the function to hold up the entire weight of the body during the single leg stance.

Foot's movements are made around 3 perpendicular axes (Figure 25): the transverse axis passing through the two malleoli (XX) influencing the movements of flexion-extension (plantar and dorsal flexion) of the foot; the longitudinal axis of the leg (Y - vertical) which influences the movements of abduction-adduc-

tion of the foot; and the longitudinal axis the foot (Z - horizontal) which conditions the orientation of the foot plant causing the pronation-supination movements [18].

In the ankle joint, the talar pulley articulates with the complementary surface of the lower tibial mortise and the facet joints of the internal and lateral malleoli. This joint is stabilized by the collateral ligaments (external/ lateral and internal/ medial, the plane surface of the latter is constituted by the deltoid ligament) and the anterior and posterior ligaments (simple capsular thickening) (Figure 26) [19].

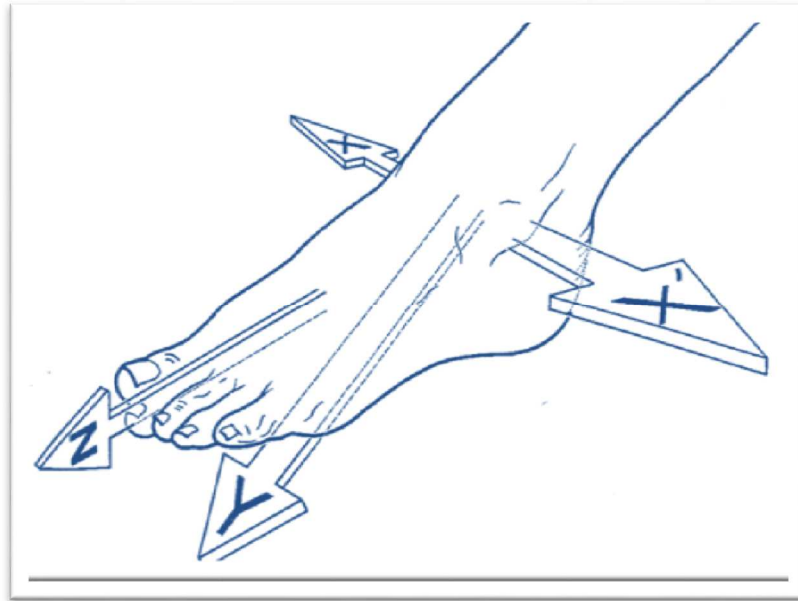


Figure 25 Foot movements around the 3axes. Source: Kapandji I.A. Fisiologia articolare, Volume 2. Arto inferiore. Società Editrice D.E.M., Roma, 1974

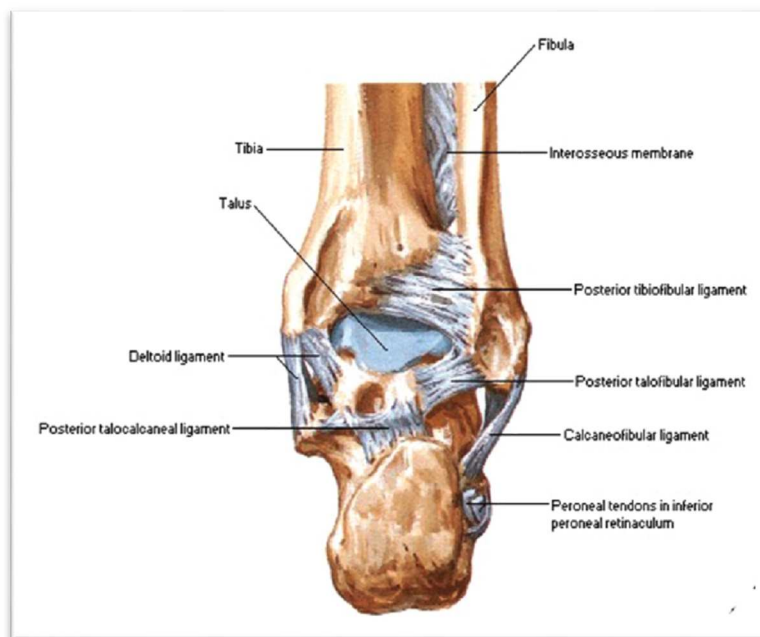


Figure 26 Anatomical view of the foot. Source: Netter F. Atlas of human anatomy. 6th edition- Elsevier

Ankle flexion- extension reaches 70-80° (20-30° of flexion and 30-50° of extension) and the bony conformation together with the capsular ligaments limit a greater excursion on the transverse axis.

The foot joints are complex and numerous, and have the function of relate the tarsal bones with the metatarsals (Figure 27-28) [19].

The intrinsic foot joints can be divided into:

- the talo-calcaneal joint (subtalar);
- the medium-tarsal joint (Chopart);
- the tarsal-metatarsal joint (Lisfranc);
- the navicular-cuboid and the navicular-cuneiform joints.

These joints have the function to guide the foot in relation to the vertical axis of the leg and around its own longitudinal axis, permitting the correct support of the foot on the ground. Additionally, they allow to modify the shape and curvature of the plantar arches adapting them to the ground roughness.

The talus and the calcaneus are connected by the subtalar articulation (Figure 29) that is made up by two artrodies; the posterior surface of the talus is applied to the Destot's thalamus (Figure 30), a wide surface placed on the top the calcaneus. It is an independent joint, enclosed by capsular-ligamentous structures; the small area of the lower face of the head and neck of the talus lays on the front surface of the calcaneus at the level of the small and large apophyses [19].

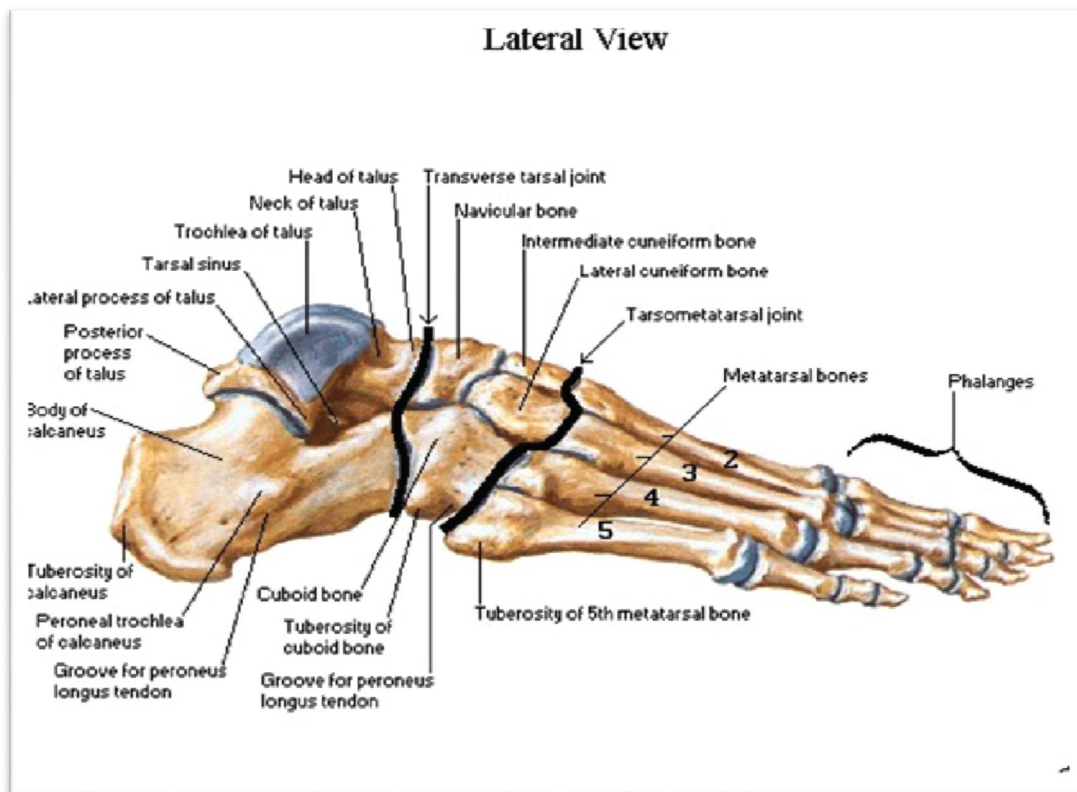


Figure 27 Lateral view of the foot. Source: Netter F. Atlas of human anatomy. 6th edition- Elsevier

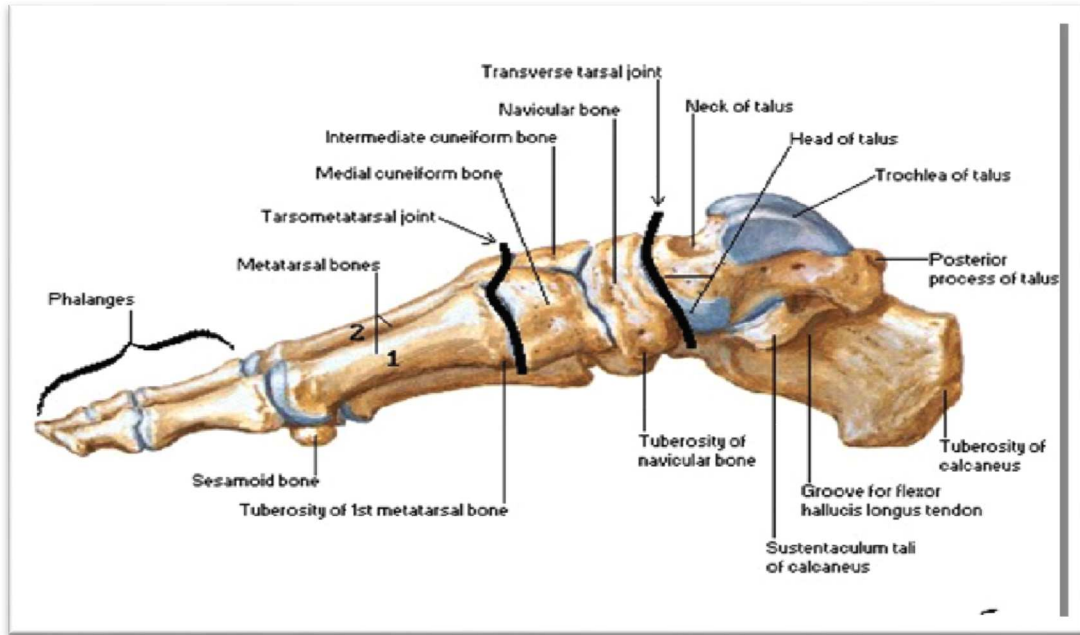


Figure 28 Medial view of the foot. Source: Netter F. Atlas of human anatomy. 6th edition- Elsevier

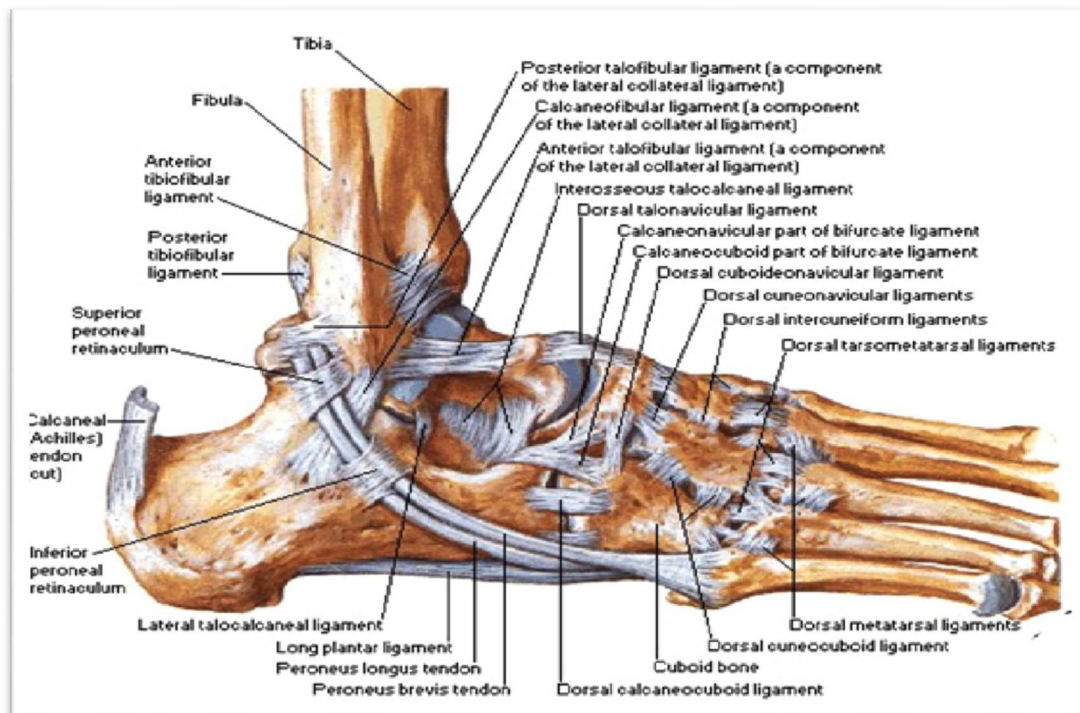


Figure 29 Lateral view of the foot. Source: Netter F. Atlas of human anatomy. 6th edition- Elsevier

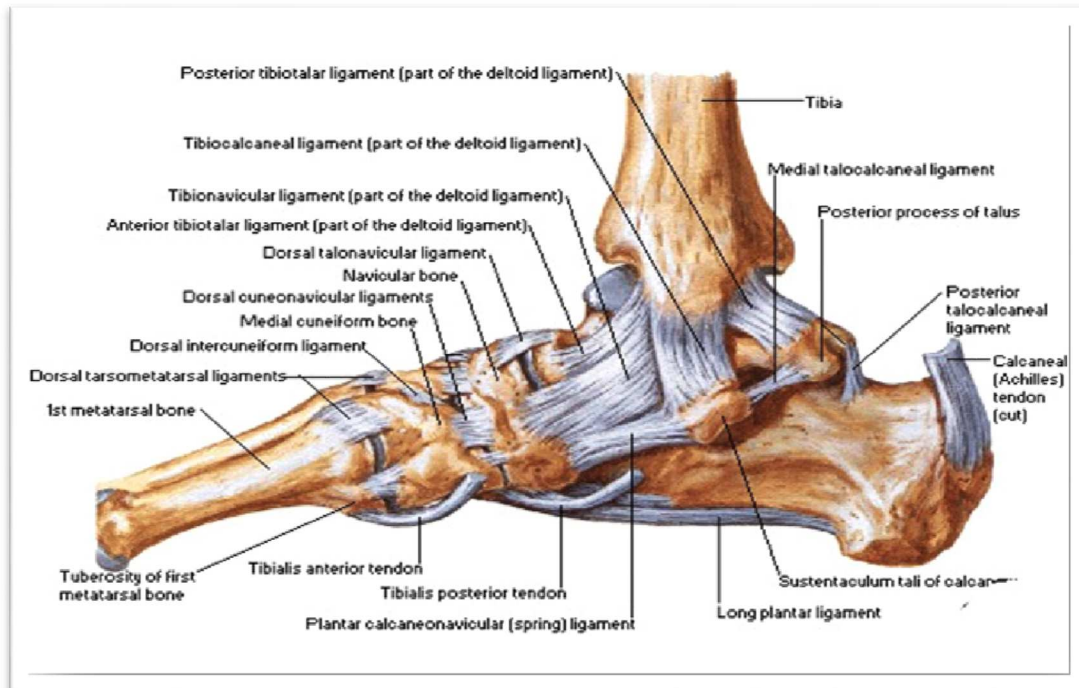


Figure 30 Medial view of the foot. Source: Netter F. Atlas of human anatomy. 6th edition- Elsevier

The subtalar joint is stabilized by the talo-calcaneal interosseous ligament, which occupies the sinus of the tarsus, and has an essential role for statics and dynamics of the subtalar joint, as it allows the distribution of the body weight (transmitted from the leg on the talus pulley) on the thalamus and the anterior surface of the calcaneus. The talus receives the stresses transmitted by the malleolus and distributes them to the other bones of the foot in 3 directions: towards the calcaneus through the thalamic surface, in the direction of the internal arc of the foot through the talonavicular joint, and in the direction of the external arc of the foot through the talocalcaneal joint.

The midtarsal joint, or Chopart's joint, is constituted by the talonavicular outline, concave on the back, and by the calcaneus-cuboid outline, concave forward (Figure 29-30): therefore it resembles an Italian S. This joint is supported by five ligaments: the glenoid ligament or calcaneal-navicular lower ligament, the talonavicular superior ligament, the Chopart's Y ligament (consisting of an internal beam, calcaneal-navicular and one external calcaneus-cuboid), the dorsal calcaneus-cuboid ligament and the plantar calcaneus-cuboid ligament [19].

The foot can perform movements around the vertical axis of the leg and around its own longitudinal axis. Around the vertical axis, on the horizontal plane adduction (toe towards inside) and abduction movements (toe towards outside) are performed; the overall range of motion is between 35° and 45°. Regarding the longitudinal axis the foot rotates so to orientate the plantar surface to the internal part in supination and outward in pronation. Practically, these movements do not exist in a pure state: abduction is coupled to supination and a slight extension determining the complex movement of inversion; adduction is accompanied by pronation and a slight flexion determining the complex movement of eversion (Figure 31) [16].



Figure 31 Foot movements around the vertical axis of the leg and around its own longitudinal axis.

Source: Kapandji I.A. *Fisiologia articolare*, Volume 2. Arto inferiore. Società Editrice D.E.M., Roma, 1974

In the upright position on a horizontal plane and in symmetric support the articular surfaces of the subtalar joint are maintained in contact by the body weight, are congruent and in a stable conformation.

In the movements of eversion, the front end of the calcaneus moves in and out and tends to lie on its inner face; the anterior facet joint at the level of the neck of the talus, and the medial facet at the level of small apophysis of the calcaneus, remain in contact forming a pivot and allowing the posterior talar articular surface to slide down and forward on the thalamus, touching the floor of the tarsal sinus and leaving uncovered the posterior superior of the thalamus.

During the inversion movement, the anterior extremity of the calcaneus tends to lie on the outer face, the facets of the pivot remain in contact, the subtalar surface rises on thalamus uncovering its anterior inferior part; the talus inversion facet (there more internal) reclines on the horizontal large apophysis of the calcaneus.

The subtalar and midtarsal joints behave as an inseparable functional unit: the complex of the hind foot. These joints together determine the equivalent of a single articulation, which implements its movement about an axis oblique to the previous ones: the axis of Henke. The movement of inversion and eversion, therefore, can be described as a simple movement of rotation about the axis of Henke, which represents the resultant of the three axes of movement, around which are realized adduction-abduction, flexion-extension and pronation-supination. Such axis penetrates through the superior-internal part of the talus neck, passes through the sinus tarsi and comes out from the posterior tuberosity of the calcaneus.

The posterior tibialis muscle inserts on the tubercle of the navicular; its contraction pulls inward and upward the bone. As a result of this displacement, the upper outer of the talar head remains uncovered and the cuboid is dragged inwards and downwards (forefoot adduction and supination) thanks to the hull-cuboidal ligaments.

During the movement of eversion, the contraction of the peroneus brevis muscle, which fits on the fifth metatarsal styloid, pulls the cuboid outwards and backwards; this drags the navicular lowering it and discovering the upper-inner part of the talar head and, therefore, the calcaneus (forefoot abduction and pronation).

The axis of Henke has a variable position; it moves during gait. Indeed, we can distinguish a location of departure and one of arrival, and a plan between these two extreme levels containing intermediate positions. At the level of the hind foot there are two axes that are not parallel: the axis of the ankle and the axis of Henke. To explain the relationship between these two axes a mechanical model of a universal joint can be used; it is "eterocinetic" as its axes are orthogonal to each other, but oblique, allowing reverse movements and eversion.

The talus-cuneiform, inter-cuneiform and tarsal-metatarsal joints are artrodies complemented by interosseous ligaments; they perform translation and opening movements of small amplitude.

The inter-cuneiform joints allow small vertical movements that change the curvature of the medial-lateral arch of the foot.

The tarsal-metatarsal joint (Lisfranc) relates the three cuneiforms and cuboid bone with the base of the five metatarsals, and is formed by artrodies. It is supported by powerful ligaments: the ligament of Lisfranc, stretched between the outer face of the first wedge and the inner face of the base of the second metatarsal, and a ligamentous system constituted from direct and cruciate fibers outstretched between the cuneiform and metatarsal bases. Moreover, on the plantar side of the base of the first metatarsal the tendon of the peroneus longus muscle attaches. The spacing of Lisfranc is skewed inside out, from superior to inferior and from front backward. It contributes to the movements of inversion and eversion. The three cuneiforms constitute a mortar in which the base of the second metatarsal fits, which has the most stable shape forming the vertex of the arch. The other metatarsals are more mobile than the second one; they have an oblique axis of flexion-extension relative to their longitudinal axis.

The metatarso-phalangeal joints permit movements of flexion-extension and movements of laterality of small amplitude. Active extension can reach 50-60°, active flexion 30-40°; passive extension, indispensable during walking, is 90°, while passive flexion is 45-50°.

Active toes extension is due to 3 muscles: an intrinsic muscle, the pedidius, and two extrinsic muscles, the extensor hallucis brevis and the extensor digitorum brevis. The pedidius muscle consists of four muscles that originate from the calcaneal part of the tarsal sinus; its four terminal tendons are confused with the tendon of the extensor of the first four toes, except the first that plugs directly to the dorsal surface of

the proximal phalanx of the hallux. It acts as an extensor of the metatarsal-phalangeal joints of the first four toes (it is considered the true extensor digitorum).

The extensor digitorum, belonging to the anterior compartment of the leg, starts on the front face of the instep and is inserted through four tendons, at the level of the last four toes. The extensor of the hallux begins with the extensor digitorum in the anterior compartment of the leg and ends on the two phalanges of the hallux.

Toes flexion is made by the deep layer of the posterior muscles of the leg and by the plantar muscles of the foot, which are arranged in three planes. The deep plane is formed by the interosseus and the muscles attached to the first and fifth toe; the dorsal interossei have an action of flexion-extension and move fingers away from the axis of the foot. The plantar interossei abducts the last three toes. The first toe is moved by the adductor and the internal flexor hallucis brevis in the inner side, and by the adductor and the head of the flexor hallucis brevis in the external side. The opponent of the fifth toe, the flexor brevis and abductor of the fifth represent the muscles moving the fifth toe.

The middle floor consists of the flexor digitorum and flexor of the hallux; the first originates in the posterior tibiae and ends on the basis of the distal phalanx of the latest four toes. Before insertion, its tendons leave a passage for the tendons of the flexor brevis. They are attached to the four lumbrical muscles; their action is flexion of the first phalanx and extension of the last two; the right flexor hallucis originates in the fibula and inserts on the second joint of the big toe.

The superficial layer contains the superficial flexor plantar brevis that originates at the level of the tuberosity posterior to the heel and ends on the second phalanx of the latest four fingers; this muscle flexes the second on the first phalanx.

The flexor muscles of the ankle are positioned anterior to the transverse axis passing through the ankle joint; they are the tibialis anterior, extensor hallucis longus and extensor digitorum. The tibialis anterior originates from the anterior surface of the tibia and the interosseous membrane and inserts on the first cuneiform and first metatarsal. The tibialis anterior and extensor hallucis longus, being located within the axis of Henke, act simultaneously as adductor and supinator muscles.

The extensor digitorum, instead, being outside of this axis, also acts as abductor and pronator. To obtain a pure bending the ankle is necessary to simultaneously contract these muscles in a balanced way.

The extensor muscles of the ankle pass behind the axis of flexion-extension of the tibio-talar joint; the most important and effective of these is the triceps, consisting of three parts: the soleus and the two gastrocnemi, that converge in a common tendon, the Achilles tendon. The soleus, mono-articular, originates from the posterior surface and proximal fibula, tibia and its fibrous arch; the gastrocnemius, medial and lateral, respectively originate from the medial and lateral femoral condyle and the corresponding condylar shell. Since they are bi-articular muscle, they have an efficacy strictly dependent on the degree of knee flexion. Knee extension moves the proximal insertion of the gastrocnemi, thus providing a passive stretch that increases their power.

The triceps surae has a complex aponeurosis system consisting of three isolated aponeuroses (origin) converging in two terminal aponeuroses: a thick foil giving rise to the Achilles tendon and a sagittal lamina perpendicular to the previous. The muscular fibers of the gastrocnemius from their origin at the femoral condyles are directed distally, forward and posterior to the leg axis. The fibers of the soleus are divided into two groups, one inserted on the posterior face of the terminal blade and one inserted on the inner face of the lamina. This arrangement of the muscle fibers recalls the spiral arrangement of the Achilles tendon. In addition to the extension of the ankle joint, the triceps determines the movement of adduction and supination, since it acts on the ankle through the subtalar joint when its contraction is pushed to the maximum.

Other muscles have a minimum extension function of the ankle, as to be considered accessory extensors: the peroneus longus and short, the tibialis posterior, flexor digitorum longus.

The peronei, going outside the axis of Henke, are also abductors and pronators. The peroneus brevis, which originates from the distal fibula and is fixed on the fifth metatarsals styloid, is especially abductor of the foot; the peroneus longus arises from the proximal fibula and it inserts on the first cuneiform and at the base of the first metatarsal. The latter acts as an extensor, in a direct manner by lowering the head of the first metatarsal (thus determining the pronation movement) and in an indirect manner acting on the metatarsals, thus allowing the triceps to act on all the foot plantar rays. It has also a role in the statics and dynamics of the plantar arch.

In addition to the tibialis anterior and the extensor of the hallux, another muscle posterior to the ankle, located outside of the axis of Henke, acts as a drafter, combining adduction and supination: the tibialis posterior. It originates posteriorly from tibia, fibula and interosseus membrane, and inserts on the tubercle of the navicular bone. The tibialis posterior work simultaneously on the ankle, the subtalar and midtarsal joints, causing the movement of inversion; it acts as adductor, attracting the scaphoid in inside, as supinator, supporting and orienting the foot thanks to its expansions on the tarsal and metatarsal bones. It also acts on the midtarsal joint lowering the navicular.

From the initial contact of the heel with the ground there is a progressive stabilization of the plantar arc and a lateral load distribution on the calcaneus-cuboid joint. After that the heel has completed the support, the subtalar joints pronate and the leg rotates inward. During the period of intermediate contact, there is a rotation of the leg outward, the start of the supination of the subtalar joint and a progressive distribution of the load on the arch side of the foot. Since the beginning of heel lift, the leg continues to rotate outward while the load is distributed on progressively on the third, second and and the first metatarsal rays.

PART 2:
THE PEDIATRIC FLAT FOOT,
PRE AND POST SURGICAL CORRECTION
3D KINEMATICS DATA

INTRODUCTION

The kinematic analysis of a body is the description of its behavior in space in terms of position and speed without reference to the forces that determine its movement.

The study of the movement of the human body has always been an important argument rising great interest. Nowadays technological progresses allow us to obtain high levels of details and accuracy in movement analysis, even for small body segments like the foot, and the parts that constitute it. Thanks to these advances, the study of the gait cycle is no longer used just for purely speculative purposes, but it has gained a very important place also in other areas. For instance, biomedical engineering can profit from individual data for the planning of functionally personalized orthotics and prosthetics; rehabilitation medicine can use gait analysis to measure the effect of neurological motor disorders affecting the lower limbs, longitudinally following up the various phases of diagnoses, treatment and rehabilitation.

Gait analysis consists on systematic measurement of the parameters characterizing the walk and can be performed using video recording, optoelectronic devices and accelerometers (kinematics), force platforms (kinetics) and electromyography (muscle activity). Each method provides different types of information, which must be interpreted by clinicians and integrated to the history and physical examination, in order to clarify the type of the movement alteration.

Nowadays, optoelectronic systems are definitely the most popular method and are used worldwide for the study of the analysis of the kinematics of the walk, but also the study of human movement in toto.

Skin markers are commonly used. In the specific case of the foot, markers are placed on precise reference points represented by the main bony prominences. Small plastic balls coated with light-reflective material are fixed with double-sided tape after accurate palpation and examination of the foot.

Special infrared-sensitive cameras are positioned along the perimeter of the area where the subject walks, and are oriented so as to be able to see the markers within the acquisition volume. Specific software provides the examiner numeric data derived from the marker trajectories detected and recorded by the cameras.

Over the years the study of the kinematics of the foot has considerably evolved.

Classical gait models for the lower limbs, which have been used in clinical practice, consider pelvis, femur and leg as separate rigid bodies. These models consider the foot as a single rigid part with a single motion vector, and only movements around the ankle joint are taken into account. The mobility that exists between the different bones composing the foot is not analyzed [20].

The complex foot-ankle is, instead, a sophisticated multi-joint system, which determines the critical interaction between the lower limb and the ground during locomotion. Therefore, the foot must be considered as a multi-segment structure, and a fruitful study of its pathologies cannot be made using standard gait analyses. Dedicated protocols should be developed.

During the last decade, various protocols for the study of foot kinematics, defined 3D models (3DMFMs), have been proposed, but most of them are referred to the foot of adult healthy patients. The most famous are the Shriners foot model, the Oxford foot model and the Milwaukee foot model [21-22].

One of the main problems in the development of a protocol for the study of the kinematics of the foot is its repeatability. In fact a solid repeatability obtained on a statistical basis is necessary to introduce a new model in clinical practice capable to be used in different gait laboratories all over the world [23].

There are several sources of error in the measurement of kinematics data.

An *intrinsic error* is an error that occurs naturally, for the simple fact that human beings are not identical in terms of anthropometric characteristics, but they also change during time; it is the *intra-subject* and *inter-subject variability*. This type of error expresses the inherent repeatability of the parameters, it cannot be correct, but only measured and taken into consideration when it is necessary to compare it with the extrinsic errors.

An *extrinsic error* is defined as the experimental error that derives from the instrumentation and the method; it comprises the *Intra-Observer and Inter-Observer variability*; these types of errors are described below.

An important element in all kinematic surveys is that a clear definition of anatomical landmarks where the markers are to be applied is a determining factor for repeatability. The error that results from improper positioning of the markers is in fact potentially very high. In addition, compared to other body segments such as the femur and the tibia, not only foot markers should necessarily be very close, but also foot intrinsic joints have more than one axis of rotation, making this kind of error crucial for a correct analysis [22].

The pediatric foot, smaller than the adult, represents an additional significant challenge: a small positioning error leads to large variations in the calculation of the joint angles. This is described in a study on the repeatability of the Oxford foot model, highlighting the increased variability of the angles between the segments in pediatric patients compared to adults [23-25].

To try to avoid these errors due to the instrumentation, several compensation techniques that are used for routine laboratory analysis of the movement can be applied: the calibration of the cameras, as well as some filtering techniques performed by processing software, can minimize the phenomenon of optical distortion. It is also important that the set-up of the laboratory is optimal: a suitable number and position of the cameras, the size of the acquisition volume. According to some estimates the accuracy and precision of the instrument should be part of the report of the data and its interpretation by the clinician.

Also, the repeatability of motion data acquired with epicutaneous markers is always under strict scrutiny, because of the movement of the skin over bony prominences where these are applied [26-28].

Despite the considerable progress that has reached movement analysis, to date its use remains controversial in clinical practice. It is now clear that the reduction of experimental extrinsic error is the primary ob-

jective. Consequently, the measurement of Intra-Observer and Inter-Observer variability helps to identify the angles and phases of the gait cycle, which are more sensitive to methodological error, and therefore require more attention.

The pediatric foot

Flexible flatfoot or pes planus valgus is a condition in which the medial longitudinal arch has normal architecture during non-weight bearing and there is a flattening of the arch during stance or weight bearing. It is characterized by calcaneal eversion, talar adduction with plantar flexion, medial arch collapse, and varying degrees of dorsolateral forefoot subluxation. This may be otherwise being termed “excessive pronation”. It is a complex deformity involving hind foot, mid foot and fore foot changes [29-30].

Infants are usually born with flexible flatfoot and do not develop a normal arch until towards the end of the second decade of life, around puberty (12-13 years). The prevalence of the flexible flatfoot varies between 21% and 57% in the population between 2 and 6 years old, while this percentage decreases to 13.4% -27.6% around the age of adolescence (12-13 years) [31-32].

Several studies of gait analysis with kinetic and kinematic data on flexible flat foot in children with an average age of 12 years have highlighted the possibility of having, in adult life, problems not only regarding foot, but also, the more proximal limb segments; for example extrarotated tibia with intrarotated femur and possible presence of misalignments and anterior knee pain with consequent alteration of the overall posture.

Traditionally, radiographic examination of the foot has been a primary assessment method to evaluate patients. Clinicians predict the functional impairment due to certain pathologies according to the change in morphology and alignment from normal anatomy as assessed by clinical examination and radiography.

However, clinicians often encounter discrepancies between symptoms of patients and their radiographic finding because static radiography does not always reflect the dynamic change of foot and ankle segments during gait. Application of dynamic functional analysis such as instrumental gait analysis can potentially be a valuable adjuvant method of clinical evaluation that may measure more accurately functional deficits.

As already pointed out, single segment conventional gait analysis, which has been used for over than 50 years and proven to be beneficial especially in neuromuscular skeletal diseases, is not ideal to evaluate foot and ankle motion because the foot segment is presented as a rigid body. During the past two decades, multiple 3-dimension multi-segment foot models (3D MFMs) have been introduced and validated enabling increased application of MFM to evaluate inter-segmental foot motions in various pathologic conditions [33-37].

Although many protocols are validated for the study of the foot in adulthood, few protocols for the study of the kinematics of the pediatric foot have been created and used in clinical practice [33-37]. The aim of this study was to determine the reproducibility of the study of the pediatric foot kinematics, establish

normality parameters and analyze foot 3D kinematic data before and after surgical correction of the flexible flat foot in children.

MATERIALS AND METHODS

The Rizzoli Foot Model

To achieve the objectives described above a foot multi-segment 3D kinematics protocol has been used, outlined by Leardini et al. in 2007 (Rizzoli Foot Model, RFM), tested and statistically validated exclusively on adults' foot [33-35]. RFM protocol considers the foot not as a single rigid segment which is articulated to the leg through the ankle, but as a set of many segments (heel, mid foot, metatarsal and hallux) which are articulated to each other, as occurs in reality.

Almost all of the following anatomical landmarks were identified with the direct placement of markers on the skin, some by calculation of the midpoint between two markers (ID, IC and IM, see below) or through calibration procedures (MM and CAB, see below, Figure 32-33):

- **PM**: the most distal and dorsal point of the head of the proximal phalanx of the hallux
- **FMB**: base of the metatarsal, dorsal medial part of the first metatarsophalangeal joint
- **FMH**: head of the metatarsal, dorsal medial part of the first metatarsophalangeal joint
- **SMB**: base of the second metatarsal, dorsal-medial part of the second metatarsophalangeal joint
- **SMH**: head of the second metatarsal, dorsal-medial part of the second metatarsophalangeal joint
- **VMB**: base of the fifth metatarsal, the dorso-lateral side of the fifth metatarsal-cuboid joint
- **VMH**: head of the fifth metatarsal, the dorso-lateral side of the fifth metatarsophalangeal joint
- **TN**: the most medial part of navicular's tuberosity
- **MC**: the most dorsal and distal part of the medial cuneiform (made to coincide with SMB)
- **TC**: the most lateral part of cuboid's tuberosity (made to coincide with VMB)
- **ID**: Center of the mid foot, intermediate point between TN and TC
- **CA**: upper part of the posterior tuberosity of the calcaneus (area of insertion of Achilles tendon)
- **CAB**: most prominent and distal posterior tuberosity of the calcaneus
- **PT**: most lateral part of the peroneal tubercle of the calcaneus
- **ST**: the most medial part of the sustentaculum tali of calcaneus
- **IC**: center of the calcaneus, midpoint between ST and PT
- **TT**: most anterior part of the tibial tuberosity
- **HF**: most proximal part of the fibular head
- **LM**: most distal part of the lateral malleolus
- **MM**: most distal part of the medial malleolus
- **IM**: center between the malleolus, midpoint between LM and MM The 3-D joint rotations were calculated between the shank, i.e. tibia and fibula, and the calcaneus (Sh-Ca), between the calca-

neus and the midfoot (Ca-Mi) and between the mid foot and metatarsus (Mi-Me). The rotation of the entire foot respect to the shank (Sh-Fo) and of the metatarsus respect to the calcaneus (Ca-Me) was also calculated. Dorsi /plantar flexion, abduction/adduction and eversion/inversion rotations were calculated at each joint in the sagittal, frontal and transverse plane respectively.

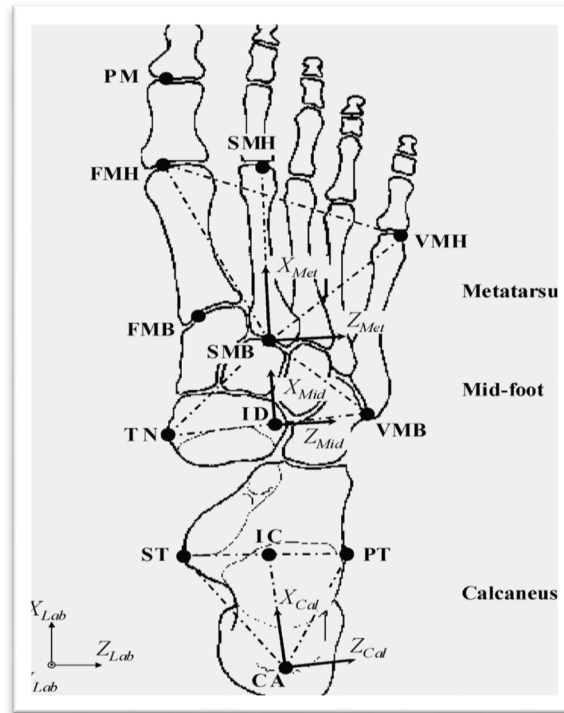


Figure 32 Diagram of the foot illustrating the location of the markers and the rigid segments



Figure 33 Spherical epicutaneous markers (diameter 10 mm) applied by double-sided adhesive tape in correspondence of the anatomical points of each foot, according to the RFM

The following planar angles in transverse (first and fifth metatarsals respect to the second) and sagittal (the first, second and fifth metatarsal bone in the laboratory frame) planes were also calculated (Figure 34):

- **F2Pt**: the angle between the projection of the FMH-PM line and the projection of the FMB-FMH line on the transverse plane, expressing valgus of the first metatarsophalangeal joint
- **S2F**: the angle between the projection of the line through FMB-FMH and the projection of the line through SMB-SMH on the transverse plane of the metatarsal
- **S2V**: the angle between the projection of the line through VMB-VMH and the projection of the line through SMB-SMH on the transverse plane of the metatarsal
- **F2G**: the angle between the projection of the line through FMB-FMH and the ground in the sagittal plane
- **S2G**: the angle between the projection of the line through SMB-SMH and ground in the sagittal plane
- **V2G**: the angle between the projection of the line through VMB-VMH and the ground in the sagittal plane
- **F2Ps**: the angle between the projection of the line through FMH-PM and the projection of the line through FMB-FMH on the sagittal plane of the metatarsus, expression of the dorsiflexion of the first metatarsophalangeal joint
- **MLA**: angle between the projection of the line through CA-ST and the projection of the line through ST- FMH on the sagittal plane of the foot, expression of the medial slipping of the navicular bone

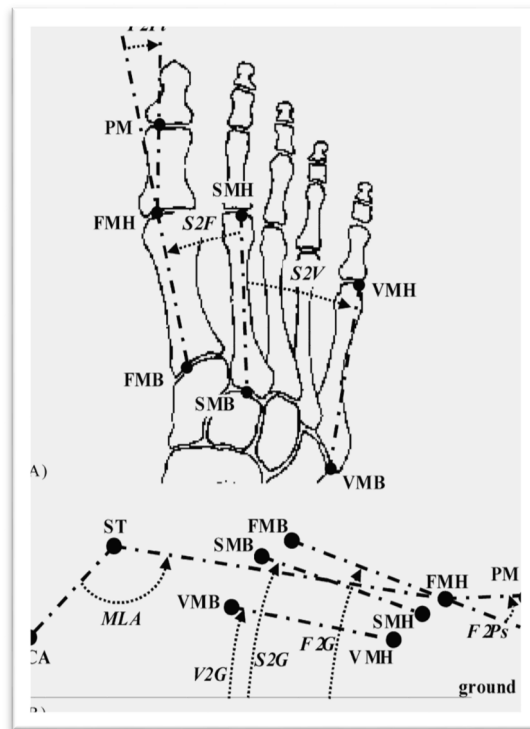


Figure 324 Calculation of the angles on the planar planes transverse (A) and sagittal (B)

Modification of the original RFM

The initial utilization of this model has revealed the need for most robust calculations, such as those relative to the first metatarsal-phalangeal joint rotation, and for measurements more consistent with clinical observations, particularly those associated to common foot deformities as in flat foot. As for the later, the most critical variables in the diagnosis are the frontal plane orientation of the calcaneus and the angle representing the medial longitudinal arch (MLA). In fact, because of the position of anatomical landmarks used to track calcaneus in the measured frontal plane, in normal feet the angle in upright neutral position was found not to be consistent with the clinical observations of 0 and 5 degrees in valgus.

Additionally, the original 2 marker-based vectors used to estimate the MLA angle did not appear to resemble exactly the corresponding traditionally X ray based measures, commonly known in the clinical setting as Meary's angle and calcaneal pitch (Figures 35-36). Modifications had to be sought to better evaluate the most common deformities typical of pes planus valgus or flatfoot [36].



Figure 35 Meary's angle –lateral view of a left (L) foot. In the normal weight bearing foot, the midline axis of the talus is in line with the midline axis of the first metatarsal. An angle $> 4^\circ$, convex downward, is considered pes planus or flat foot, an angle of 15° - 30° is considered moderate and $>30^\circ$ severe.



Figure 36 A line is drawn from the plantar-most surface of the calcaneus to the inferior border of the distal articular surface. The angle between this line and the transverse plane (line from the plantar surface of the calcaneus to the inferior surface of the V metatarsal head) is the calcaneal pitch. a decreased calcaneal pitch is considered in pes planus or flat foot. Normal range of this angle is considered between 18 - 20° , although measurements ranging from 17° to 32° have been reported as normal.

The first modification to the original RFM is related to the definition of a new anatomical reference frame for the proximal phalanx of the hallux; this was established by the location of 3 markers: PM on the head of the proximal phalanx; FMH, on the head of the first metatarsal, and VMH, on the head of the fifth metatarsal. The vertical axis (Y) was defined as the vector orthogonal to the plane passing through the 3 markers, the antero-posterior axis (X) was the line segment FMH-PM and the medial-lateral axis (Z) was the vector product of the other two. A joint coordinate system was defined to determine 3D angles be-

tween the hallux and the metatarsus segments (Met-Hal joint), the later being identified by the position of FMH, VMH and SMB, as in the original model [36].

The second modification concerned the eversion/inversion offset angle of the calcaneus with respect to the shank. This modification, which concerns the static calibration, entailed the use of an additional marker (HL) on the most distal point of the attachment area of the Achilles tendon on the calcaneus. A new frontal –plane offset for the Sh-Ca joint was defined as the angle between the line segment Ca-HL projected in the frontal plane of the shank, and the shank vertical axis in up right double-leg static posture [36].

A third modification involved the MLA angle. This was here defined as the angle between the projections, into the sagittal plane of the foot, of the line segments between St and FMH and between St and Cap. The latter point is identified by the vertical projection of the CA on the ground in the up right posture, and it is then tracked during walking by a technical reference frame based on the 3 markers on the calcaneus. Such modification was intended to achieve better consistency with the rear foot orientation and with clinical and radiographic definitions. By doing so, the newly defined MLA angle may be described as a compromise between the radiographic angle of Meary and calcaneal pitch [36].

The institutional review board of the Humanitas Research Hospital approved this study and all participants (parents/ legal guardians as well as children) gave a proper informed consent.

Inclusion and exclusion criteria

The inclusion criteria were the same for both groups:

- children aged from 12 to 14 years;
- children with both feet to be corrected surgically (only for children candidate to surgery);
- children with normal body mass index (B.M.I.).

The exclusion criteria were:

- children with concomitant systemic diseases;
- children with clinical signs of joint laxity;
- children who practice sports at a competitive level, to prevent the onset of problems related to the overuse of the foot due to the increasing demands that sport needs.

According to such criteria, the study population was composed of 2 groups: 10 children (20 feet, 5 males and 5 females, shoe size range 37-44, mean age 13.1 ± 0.8 years, height 162.2 ± 10.6 cm, weight 48.4 ± 10.7 kg) without any disorders of the foot were evaluated to obtain normal reference data, and 20 children with bilateral flexible flatfoot candidate to bilateral surgical correction (40 feet, 13 males and 7 females with a mean age of 13.3 ± 0.8 years, height 161.2 ± 8.6 cm, weight 45.4 ± 10.6 , shoe size range 38-43).

Clinical and instrumental assessment

The clinical, radiographic and instrumental evaluation of patients was performed preoperatively and at a distance of 12 months by the same surgeon who performed surgery, to limit any errors related to individual variability.

The trajectories of the markers were acquired by a system for motion capture and a modified Rizzoli Foot Model (RFM) as described above [35].

Participants performed a 5-minute warm up protocol of comfortable walking. After warming up, each subject had 16 spherical epicutaneous markers (diameter of 10 mm - Fig. 1) applied by double-sided adhesive tape in correspondence of the anatomical points of each foot, according to the LMF protocol. A single experienced operator, to limit errors related to individual variability, performed markers placement.

At first, static data were obtained in a calibration trial with the foot flat on the ground. After verifying that all markers were displayed correctly, those corresponding to the medial malleolus and the calcaneus (defined MM and CAB) were removed. After the calibration trial, subjects were asked to walk at a comfortable speed along a straight line within the acquisition volume. Gait data were collected using the 6 cameras of an optical motion capture system (Vicon Bonita B10, Vicon Motion System Ltd Oxford, UK). Kinematic data were collected and tracked using the foot 3D-RFM software. Three representative strides from 5 separate trials were selected, and the mean values were used for the analysis.

The whole gait cycle was divided into 100 time points with 1% interval and inter-segmental data were collected at each time point. The following segments were considered as rigid: leg (including tibia and fibula), foot in toto (including all the bones), heel, mid foot (which includes the navicular, the three cuneiforms and cuboid) and the metatarsal (which includes the five metatarsal bones); the proximal phalanx of the hallux, the 1st, 2nd and 5th metatarsal bones were considered as independent segments.

All instruments, excluding X-rays, are not invasive, and do not bear any discomfort to the subjects.

Standard radiographs of the feet in load in two projections (anterior-posterior and lateral-side), the axial view of the heel, were performed preoperatively and 12 months after surgery and measurements of the calcaneal pitch angle, talo-navicular coverage (Figure 37) and Meary's angle were performed according to the good clinical practice. Radiographs were not requested for the participants who did not undergo surgery because radiological expose without any clinical motivation is ethically incorrect.

The same surgeon clinically and/or radiographically evaluated all participants.



Figure 37 Normal talo navicular coverage angle- anterior posterior views.
The angle between the articular surfaces of the talus and the navicular is less than 7°.

Surgical Technique

For all patients undergoing surgical correction, an arthroereisis of subtalar joint (calcaneus-stop) was performed by the same surgeon. For all patients, mean time between surgical corrections of both feet was 6 months.

Under seduction and through a percutaneous approach, centered on the tarsal sinus (about 1 cm- Figure 38), its floor is reached, and, under fluoroscopy, a metal screw (titanium-Orthofix- Figures 39-40) was implanted. Patients were discharged after a 2-3 hours rest. Walking was possible immediately after surgery, but sport was allowed only after 30 days.



Figure 38 Percutaneous incision (about 1 cm) centered on the tarsal sinus

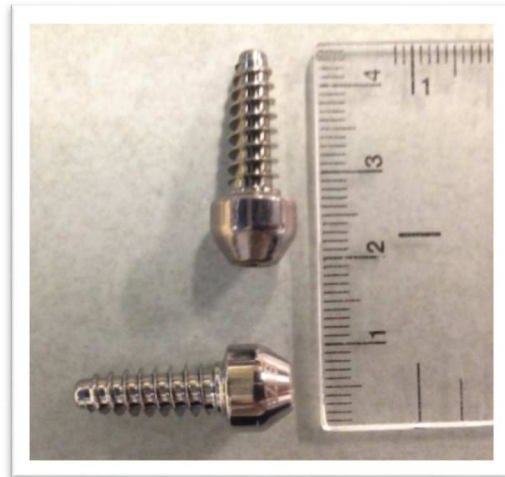


Figure 39 Small dimension metal screw (titanium-Orthofix)



Figure 40 X ray of the foot (lateral view) before and after arthroereisis of the subtalar joint

Statistical analysis of the data

For all statistical comparisons the Wilcoxon test for parametric and non parametric data was used and p values < 0.05 were considered statistically significant. Patients were divided in 3 groups:

1. normality group
2. before surgery group
3. after surgery group

For all the variables and for the three planes (x : sagittal; y : frontal; z : transverse) of the space the following comparisons were performed:

- (1) versus (2)
- (1) versus (3)
- (2) versus (3)

RESULTS

Definition of normality values

3D rotation of the joints: are graphically represented in figure 41.

Leg in toto - Foot in toto (ankle Sh-Fo)

The sagittal plane motion data are very consistent, from an average of $6^\circ \pm 2^\circ$ of plantar flexion during the loading response, to an average of $7^\circ \pm 2^\circ$ of dorsal flexion in the terminal phase of stance. In the frontal plane the foot is in inversion (adduction, plantar flexion and supination) of $5^\circ \pm 4^\circ$ at its initial contact with the ground, followed by eversion (abduction, dorsal flexion and pronation) during load, and again in inversion of $4^\circ \pm 4^\circ$ in the terminal stance phase. In the transverse plane, the foot remains roughly neutral to the terminal phase of the stance, with an abduction of $10^\circ \pm 5^\circ$ (pre-swing).

Leg in toto – Calcaneus (Sh-Ca)

In all three planes of the space the pattern of movement of the articulation follows the leg in toto - Foot in toto movement, however, are performed with a narrower articular range in the transverse plane (adduction of $5^\circ \pm 3^\circ$ in the pre- swing)

Calcaneus – Mid foot (Chopart joint)(Ca-Mi)

In all three planes a reduced joint range of movement is observed; in the terminal phase of stance the mid foot is dorsiflexed ($7^\circ \pm 3^\circ$), in inversion of $5^\circ \pm 3^\circ$ (relative to the entire phase of stance when it was in eversion) and adducted ($3^\circ \pm 4^\circ$) respect calcaneus.

Midfoot - Metatarsus (Lisfranc joint)(Mi-Me)

A reduced joint range of motion occurred at the level of this articulation in all three planes of space, including the frontal, where there is no inversion in the terminal phase of the stance.

Calcaneus – Metatarsus (Ca-Me)

Initial inversion of $2^{\circ} \pm 5^{\circ}$ in the frontal plane in the phase of the loading response, followed by a realignment in the mid stance and eversion of $9^{\circ} \pm 3^{\circ}$ at the time of toe-off.

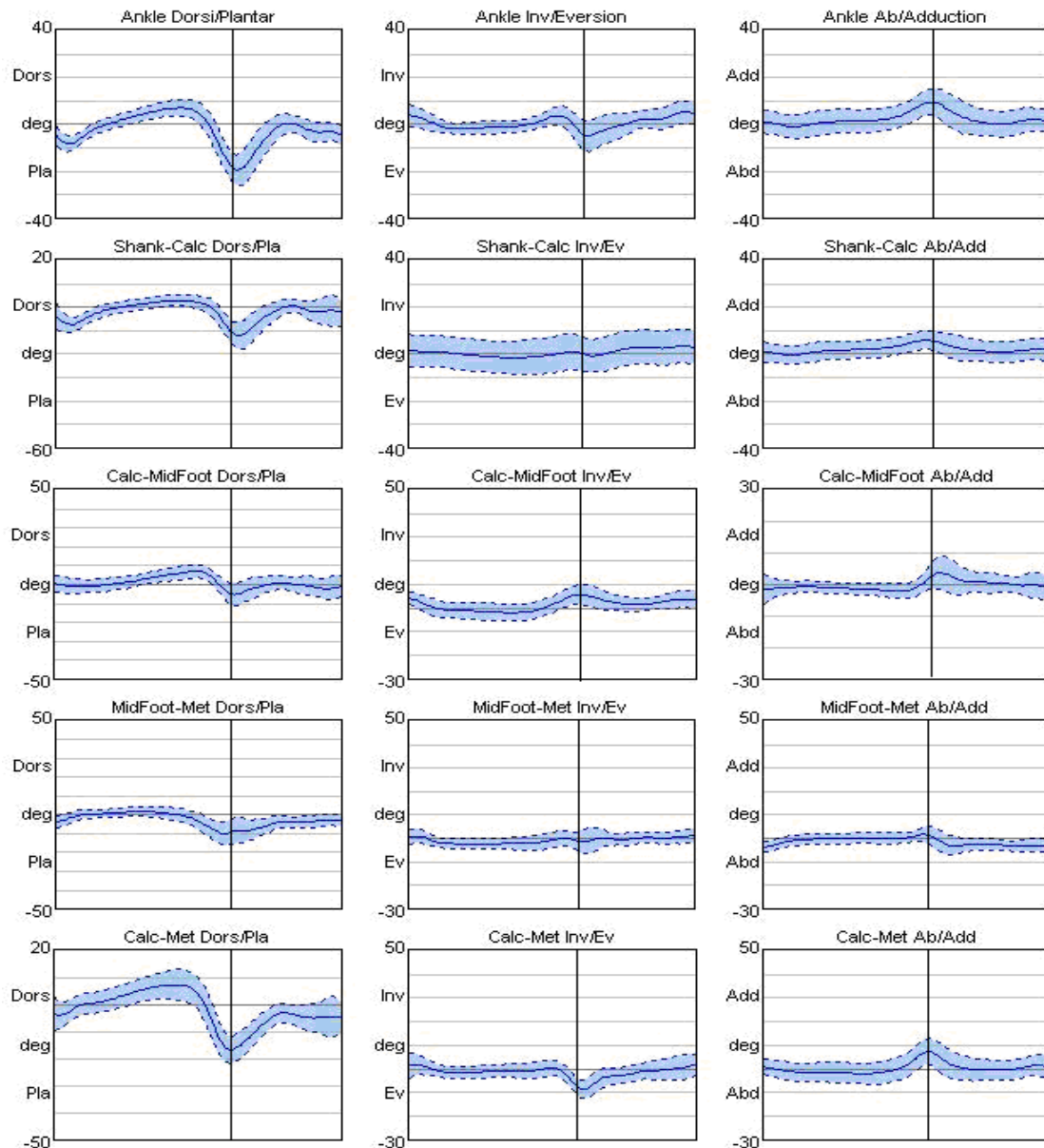


Figure 41: joints rotations on the 3 planes are represented in the three columns (sagittal, frontal and transverse respectively) and the five segments along the five lines. The mean values (blue line) and the standard deviation (blue dash dot lines) are calculated during the entire gait cycle. Degrees of each variable are represented on the ordinate axis, while phases of the gait cycle are represented at the abscissa axis. The black vertical line indicates the toe off phase (60% of the gait cycle)

Planar angles: are graphically represented in figures 42 and 43.

F2Pt (1st metatarsal versus hallux-transverse plane)

It is the angle between the straight line passing through the major axis of the metatarsus and the straight line passing through the major axis of the hallux in toto, expressing the valgus of the first metatarsophalangeal joint. At heel strike, this angle is in adduction (varus) of $6^\circ \pm 5^\circ$ becoming subsequently neutral until the end of stance, when returns in adduction of $10^\circ \pm 5^\circ$ at the final phase of toe-off.

S2P (1st versus 2nd metatarsal-transverse plane)

It is the angle between the straight line passing through the major axis of the first metatarsal bone and the line passing through the major axis of the second metatarsal bone. For the whole duration of the stance phase the angle is approximately neutral, converging of few degrees ($3^\circ \pm 5^\circ$) at the terminal stance.

S2V (2nd versus 5th metatarsal-transverse plane)

It is the angle between the straight line passing through the major axis of the second metatarsal bone and the line passing through the major axis of the fifth metatarsal. It is observed that with the increase of the percentage of stance, the angle amplitude also increases. This is due to the divergence of the metatarsals heads under load during the propulsion phase (up to $4^\circ \pm 3^\circ$), and then converging again in the swing phase.

F2G, S2G and V2G (1st, 2nd, 5th metatarsal versus ground respectively- sagittal plane)

These are the angles obtained respectively between the first, the second and the fifth metatarsal bone relative to the ground and are extremely consistent, because of the low standard deviations for the entire duration of the gait. The three metatarsal bones have an orientation with the heads upward for the first 20% of the stance until the moment of the complete contact of the foot; then, remain in a neutral position up to 70% of the stance when angling down. The angle V2G is one that has the major range of motion relative to the others.

F2Ps (1st metatarsal versus hallux- sagittal plane)

It is the angle between the straight line passing through the major axis of the first metatarsal bone and the major axis of the hallux in toto. It is neutral at the moment of the contact with the ground, then there is a hallux plantar flexion (up to $10^\circ \pm 5^\circ$) during the loading response and mid-stance, while, in the propulsive phase, a rapid dorsal flexion (up to $45^\circ \pm 10^\circ$) is observed.

MLA, Medial Longitudinal Arch (sagittal plane - relative to the ground)

It is the angle between the straight line passing through the major axis of the calcaneus and the straight line passing through the major axis of the first metatarsal bone. It provides roughly the same information given by the radiographic measurement of the Meary's angle in the lateral view. The MLA angle has a characteristic "double bump" pattern: in the first phase of contact of the foot to the ground and load response, an increase of $4^\circ \pm 4^\circ$ in the amplitude of this angle is observed, followed by a reduction of its am-

plitude in the support phase of about $10^{\circ} \pm 5^{\circ}$ due to the contraction of muscles and the plantar fascia opposing the force exercised by the body's weight. In the terminal stance, a further MLA increase is observed, followed by its new rapid reduction in the pre-swing, due to the plantar muscles and plantar fascia activation tending the arch of the foot for the toe-off.

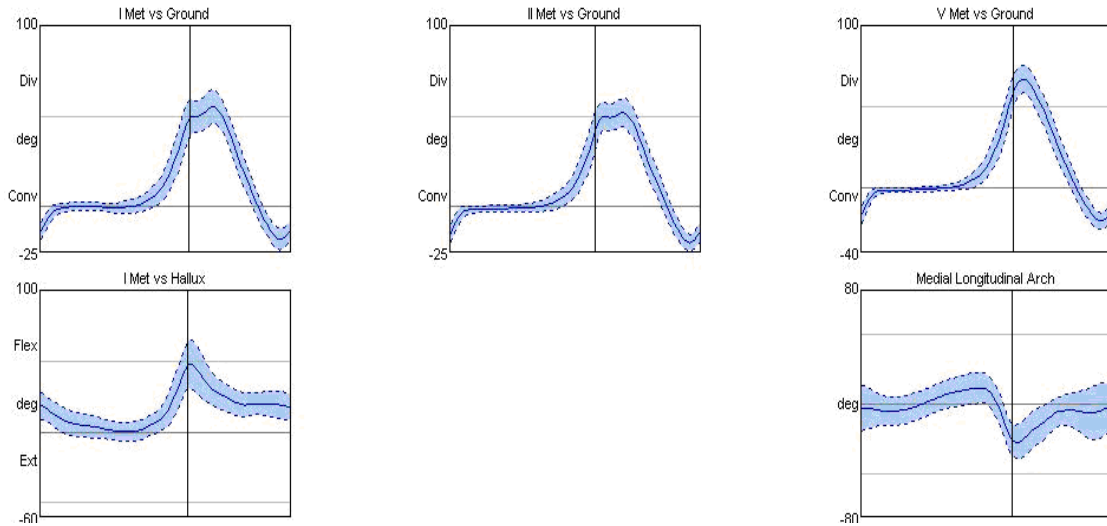


Figure 42: planar angles on the sagittal plane. The mean values (blue line) and the standard deviation (blue dash dot lines) are calculated during the entire gait cycle. Degrees of each variable are represented on the ordinate axis, while phases of the gait cycle are represented at the abscissa axis. The black vertical line indicates the toe off phase (60% of the gait cycle).

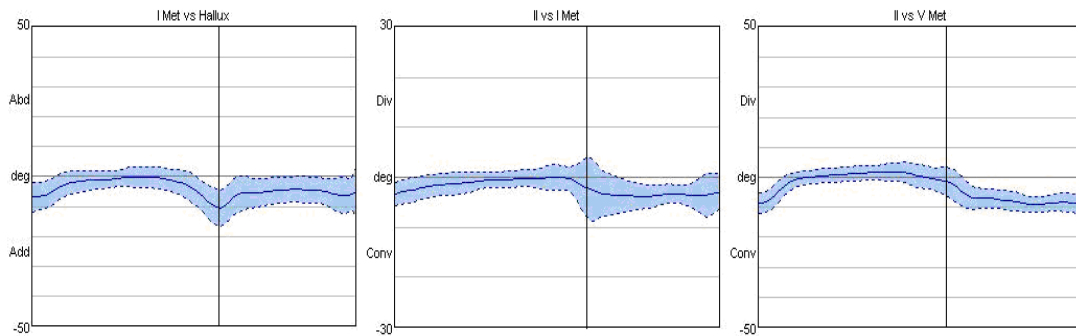


Figure 43: planar angles on the transverse plane. The mean values (blue line) and the standard deviation (blue dash dot lines) are calculated during the entire gait cycle. Degrees of each variable are represented on the ordinate axis, while phases of the gait cycle are represented at the abscissa axis. The black vertical line indicates the toe off phase (60% of the gait cycle).

Kinematic data before and after surgical correction of the foot, at the static up-right position

To obtain an easier interpretation, box plots have been created from the gained results, where:

- blue boxes represent before surgery values;
- red boxes represent after surgery values;
- top and bottom margins of each box represent the third and first quartile respectively;
- solid line inside each box represent the median or second quartile;
- colored dots represent the outliers of each group;
- horizontal dash-dot lines represents the range of normal values of each variable;
- horizontal solid black line represents the median of normal values;
- x, y, z : sagittal, frontal, and transverse planes respectively;
- all variables are given in degrees (ordinate axis).

3D rotation of the joints: values of the joints are represented in the box plots, Figure 44, while the statistical analysis, after comparison of the different groups, is shown in Table 1.

Sh-Fo segment:

- in the sagittal plane (x), despite the statistically significant difference found between the before surgery and normality groups, no difference is observed before and after surgical correction. A larger intra-sample variability with a less homogeneous distribution is observed after surgery respect to the pre surgical assessment, with the post surgical median values closer to the normality (median: before surgery, -10.5° ; post surgery, -10.15° ; normality, -7.24°);
- in the frontal plane (y), despite the statistically significant difference between before surgery and normality, no difference is observed before and after surgical correction. No differences regarding the intra-sample variability is observed before and after surgery, and distribution of the sample is the same in both cases. The post surgical median values are closer to normality than the pre surgical ones (median: pre surgery, 7.2° ; post surgery, 8.05° ; normality, 10.75°);
- in the transverse plane (z), no statistically significant difference is observed between before surgery and normality, while a difference is observed between before and after surgical correction. A reduced intra-group variability and a more homogeneous distribution is observed after surgery, relative to the pre surgical assessment. The post surgical median values are higher than those of normality (median: pre surgery, 3.45° ; post surgery, 8.1° ; normality, 3.95°).

Sh-Ca segment:

- in the sagittal plane (x), a statistically significant difference is observed between before surgery and normality, and before and after surgical correction. A higher intragroup variability with a more homogeneous distribution of the sample is observed after surgery respect to the pre surgi-

cal assessment. The post surgical median values are closer to the normality (median: pre surgery, -33.6°; post surgery, -29.7°; normality, -20.85°);

- in the frontal plane (y), statistically significant differences are observed between before surgery and normality ($p = 0.0001$), before and after surgical correction ($p < 0.0001$). A somewhat more homogeneous distribution of the sample is observed after surgery, respect to the pre surgical assessment. The post surgical median values are closer to those of normality (median: pre surgery, -10.95°; post surgery, -4.1°; normality, 4.4°);
- in the transverse plane (z), no statistically significant difference is observed between before surgery and normality, while a difference is observed between before and after surgical correction. The post surgical median values are closer to those of normality (median: pre surgery, 5°; post surgery, 7.6°; normality, 4.4°). A small part of the sample over exceed the maximum value of the range of normality (normality: 16°; post surgery, 20.5°).

Ca-Mi segment:

- in the sagittal plane (x), statistically significant differences are observed between before surgery and normality, before and after surgical correction. A higher variability with a less homogeneous distribution of the sample is observed after surgery, respect to the pre surgical assessment. The post surgical median values are closer to those of normality (median: pre surgery, 75.3°; post surgery, 62.8°; normality, 43.65°);
- in the frontal plane (y), a statistically significant difference is observed between before surgery and normality, but not between before and after surgical correction ($p = 0.9946$). A higher variability with a less homogeneous distribution of the sample is observed after surgery, respect to the pre surgical assessment. The post surgical median values are somewhat furthest from those of normality (median: pre surgery, 7.45°; post surgery, 5.55°; normality, 11.75°);
- in the transverse plane (z), statistically significant differences are observed between before surgery and normality, before and after surgical correction. A more homogenous distribution of the sample is observed after surgery, respect to the pre surgical assessment. The post surgical median values are closer to those of normality (median: pre surgery, -11.2°; post surgery, -5.7°, normality, -0.9°).

Mi-Me segment:

- in the sagittal plane (x), no statistically significant difference is observed between before surgery and normality, while a difference is observed between before and after surgical correction. Less variability with a more homogeneous distribution of the sample is observed after surgery, respect to the pre surgical assessment. The post surgical median values are furthest from normality (median: pre surgery, -70°; post surgery, -73.85°; normality, -64.65°);
- in the frontal plane (y), statistically significant differences are observed between before surgery and normality, before and after surgical correction. Less variability and a more homogeneous distribution of the sample is observed after surgery, respect to the pre surgical assessment. The

post surgical median values are closer to those of normality (median: pre surgery, 3.6°; post surgery, 9.6°; normality, 7.75°). A small part of the sample exceed the maximum values of the range of normality (normality, 16.7°; post surgery, 19.9°);

- in the transverse plane (z), statistically significant differences are observed between before surgery and normality, before and after surgical correction. A higher variability with a less homogeneous distribution of the sample is observed after surgery, respect to the pre surgical assessment. The post surgical median values are closer to those of normality (median: pre surgery, 3°; post surgery, -3.25°; normality, -4.9°). A small part of the sample exceed the maximum values of the range of normality (normality, 11.1°; post surgery, 12°).

Ca-Me segment:

- in the sagittal plane (x), statistically significant differences are found between before surgery and normality, before and after surgical correction. A higher variability with a less homogeneous distribution is of the sample observed after surgery, respect to the pre surgical assessment. The post surgical median values are closer to those of normality (median: pre surgery, 5.65°; post surgery, -13.55°; normality, -23.2°);
- in the frontal plane (y), no statistically significant differences are observed between before surgery and normality, before and after surgical correction. A similar intrasample distribution is observed both before and after surgery. The post surgical median values are closer to those of normality (median: pre surgery, 15.75°; post surgery, 15.55°; normality, 15.35°);
- in the transverse plane (z), no statistically significant differences are observed between before surgery and normality, before and after surgical correction. A higher variability with a less homogeneous distribution of the sample is observed after surgery, respect to the pre surgical assessment. The post surgical median values are closer to those of normality (median: pre surgery, 3.1°; post surgery, 2.7°; normality, 7.5°).

		Comparisons			
		axis	1 vs 2	2 vs 3	1 vs 3
Sh-Fo	x	0.0001	0.2617	0.0059	
	y	0.0106	0.9625	0.0287	
	z	0.7066	0.0005	0.0161	
Sh-Ca	x	0.0000	0.0039	0.0004	
	y	0.0001	0.0000	0.5051	
	z	0.8019	0.0005	0.0392	

		Comparisons			
		axis	1 vs 2	2 vs 3	1 vs 3
Ca-Mi	x	0.0000	0.0000	0.0000	
	y	0.0027	0.9946	0.0013	
	z	0.0002	0.0027	0.2068	
Mi-Me	x	0.0677	0.0445	0.0011	
	y	0.0171	0.0007	0.4659	
	z	0.0144	0.0201	0.5001	

Table 1: results after comparison between the different groups. Significant p values are shown in bold in grey cells. (1: normality; 2: before surgery; 3: after surgery; x : sagittal plane; y : frontal plane; z : transverse plane; vs: versus)

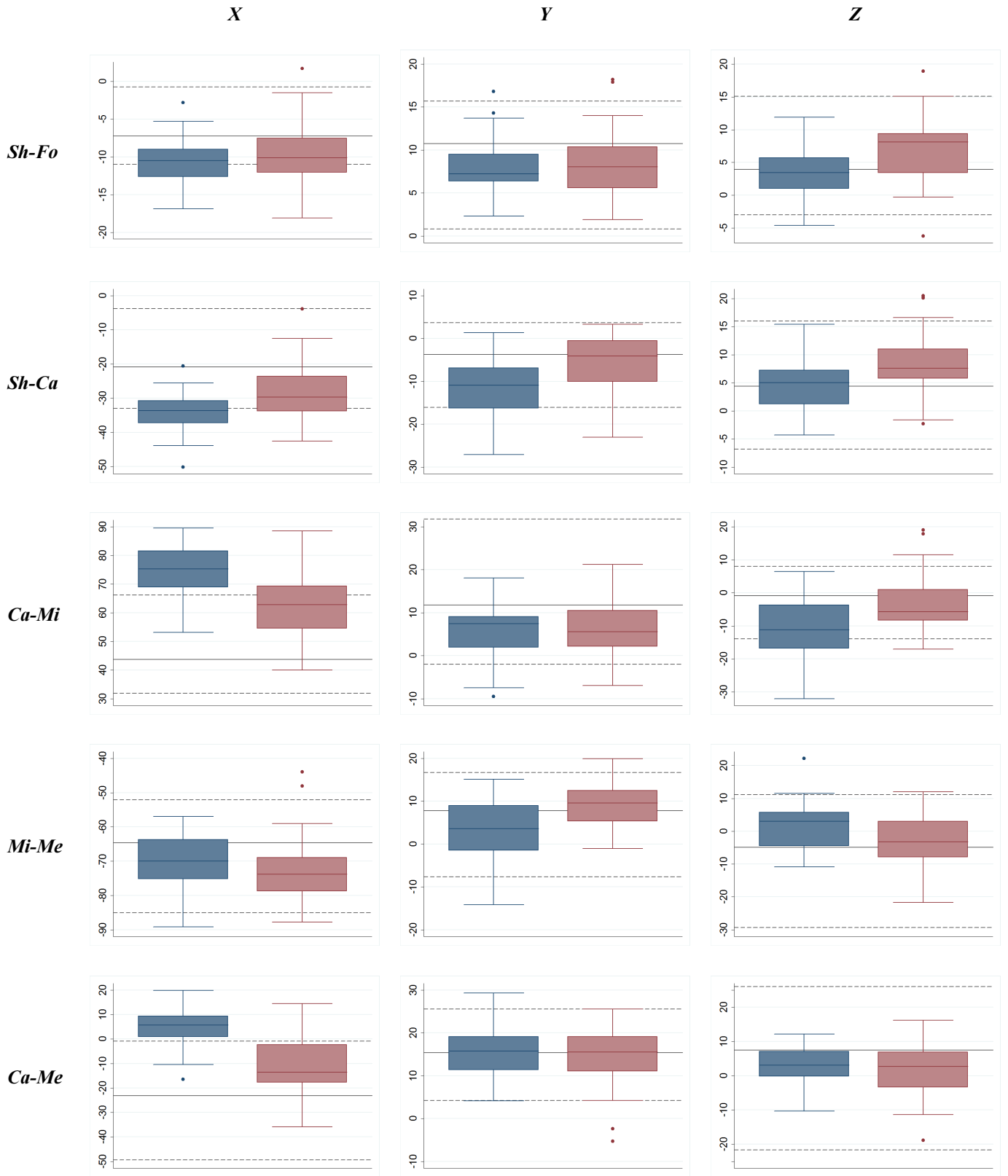


Figure 44 3D Rotational joints are represented in the first column. Blue and red boxes represents before and after surgery values. X, Y, and Z: sagittal, frontal and transverse plane. Dash-dot horizontal lines: range of normality. Solid line: median values of each group. Colored dots: outliers of each group. (+) / plantiflexion (-) are measured in the x plane, inversion (+) / (eversion (-) in the y plane and abduction (+) / adduction (-) in the z plan

Planar angles: values are represented in the box plots, Figure 45, while the statistical analysis, after comparison of the different groups is shown in Table 2.

1st metatarsal versus Hallux:

- in the sagittal plane (x), a statistically significant difference is observed between before surgery and normality, but not between before and after surgical correction. Higher variability with a less homogeneous distribution of the sample is observed after surgery, respect to the pre surgical assessment. The post surgical median values are furthest from those of normality (median: pre surgery, 2.7°; post surgery, 6.3°; normality, -0.2°);
- in the transverse plane (z), no statistically significant difference is observed between before surgery and normality, before and after surgical correction. Less variability with more homogeneous distribution of the sample is observed after surgery, respect to the pre surgical assessment. The post surgical median values are furthest from those of normality (median: pre surgery, 9.7°; post surgery, 12.45°; normality, 7.8°).

1st metatarsal versus 2nd:

- in the transverse plane (z), statistically significant differences are observed between before surgery and normality, before and after surgical correction. Higher variability with a less homogeneous distribution of the sample is observed after surgery, respect to the pre surgical assessment. The post surgical median values are furthest from those of normality (median: pre surgery, 1.3°; post surgery, -8.3°; normality, 5.85°).

2nd metatarsal versus 5th:

- in the transverse plane (z), no statistically significant differences are observed between before surgery and normality, before and after surgical correction. Higher variability with a less homogeneous distribution of the sample is observed after surgery, respect to the pre surgical assessment. The post surgical median values are furthest from those of normality (median: pre surgery, 1.8°; post surgery, 2.5°; normality, -0.15°)

1st metatarsal versus ground:

- in the sagittal plane (x), a statistically significant difference is observed between before surgery and normality, but not between before and after surgical correction. Less variability with a more homogeneous distribution of the sample is observed after surgery, respect to the pre surgical assessment. The post surgical median values are furthest from those of normality (median: pre surgery, 19.45°; post surgery, 20°; normality, 12.45°).

2nd metatarsal versus ground:

- in the sagittal plane (x), statistically significant differences are observed between before surgery and normality and before and after surgical correction. Less variability with a more homogeneous distribution of the sample is observed after surgery, respect to the pre surgical assessment.

The post surgical median values are furthest from those of normality (median: pre surgery, 20.3°; post surgery, 25.2°; normality, 24.4°).

5th metatarsal versus ground:

- in the sagittal plane (*x*), statistically significant differences are observed between before surgery and normality and before and after surgical correction. Higher variability with a less homogeneous distribution of the sample is observed after surgery, respect to the pre surgical assessment. The post surgical median values are closer to those of normality (median: pre surgery, 1.1°; post surgery, 4.95°; normality, 5.4°).

MLA:

- in the sagittal plane (*x*), statistically significant differences are observed between before surgery and normality and before and after surgical correction. Higher variability with a less homogeneous distribution of the sample is observed after surgery, respect to the pre surgical assessment. The post surgical median values are furthest from those of normality (median: pre surgery, 187°; post surgery, 168°; normality, 157°).

		Comparisons		
Planar angles	Axis	1 vs 2	2 vs 3	1 vs 3
1 st met vs Hallux	<i>x</i>	0.0259	0.0738	0.0175
	<i>z</i>	0.4330	0.6190	0.0903
1 st vs 2 nd met	<i>z</i>	0.0370	0.0000	0.1930
2 nd vs 5 th met	<i>z</i>	0.3117	0.9571	0.3548
1 st vs Ground	<i>x</i>	0.0059	0.0706	0.0001
2 nd vs Ground	<i>x</i>	0.0000	0.0000	0.2861
5 th vs Ground	<i>x</i>	0.0027	0.0001	1.0000
MLA	<i>x</i>	0.0010	0.0000	0.3231

Table 2. Results after comparison between the different groups. Significant *p* values are shown in bold in grey cells. (1: normality; 2: before surgery; 3: after surgery; *x*: sagittal plane; *z*: transverse plane; vs: versus; met: metatarsal bone)

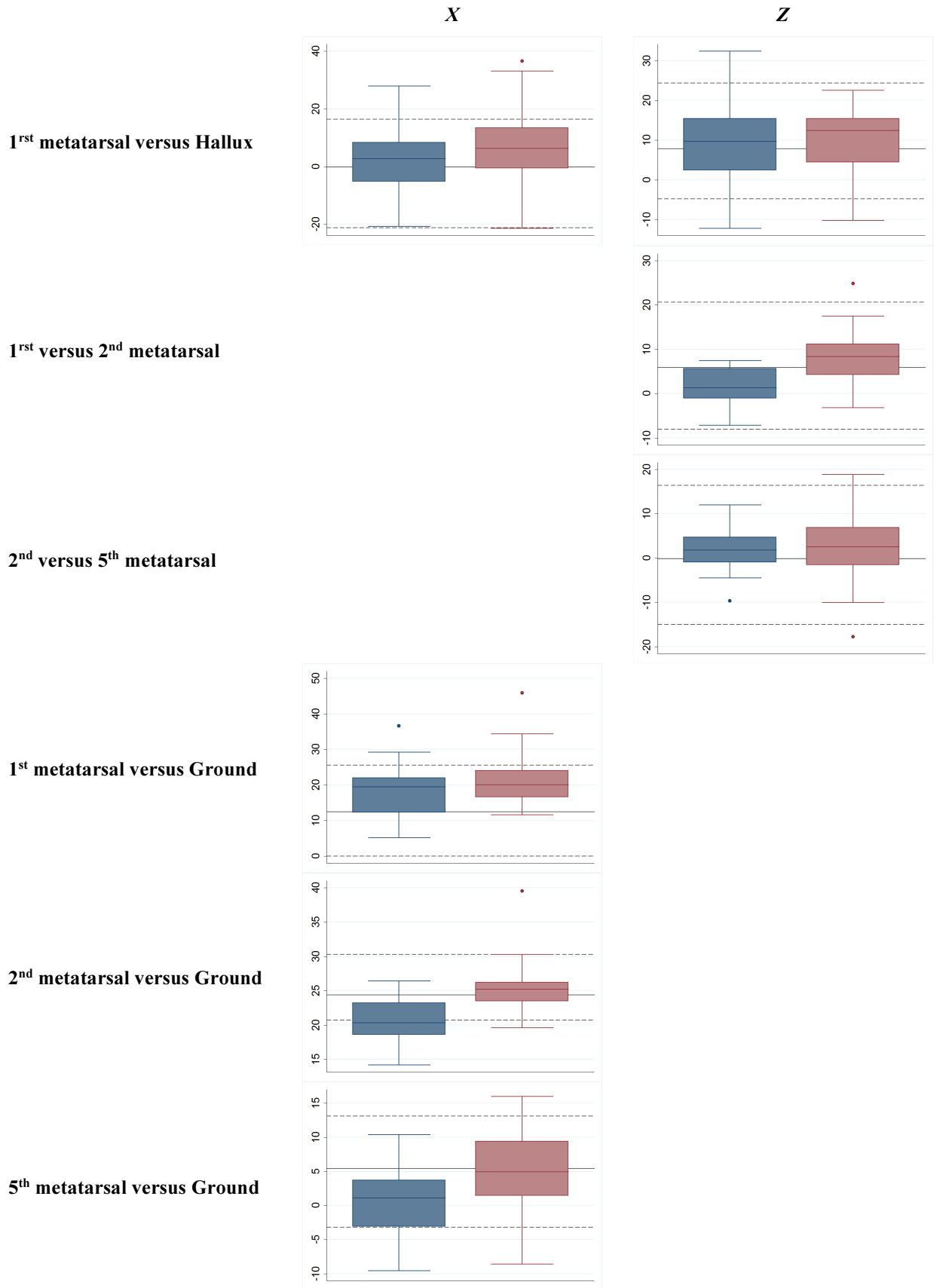


Figure 45 – see following page

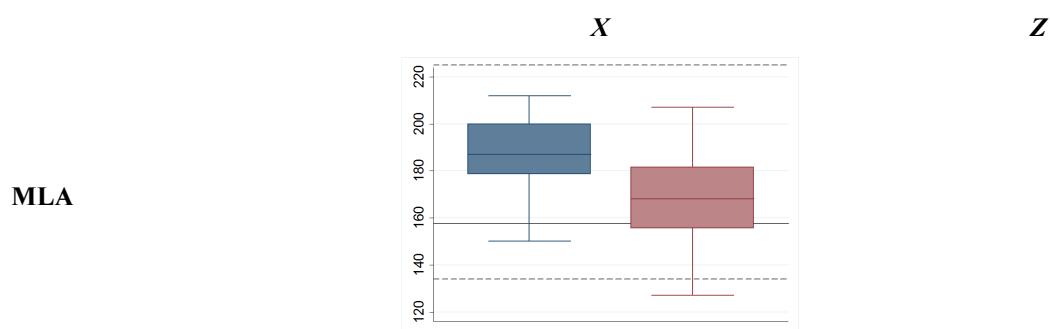


Figure 45 Planar angles are represented in the first column. Blue and red boxes represents before and after surgery values respectively; X: sagittal plane; Z: transverse plane; dash dot horizontal lines: range of normality. Solid line: median values of each group. Colored dots: outliers of each group. Dorsiflexion (+) / plantiflexion (-) are measured in the x plane and abduction (+) / adduction (-) in the z plane, except for the 1st versus 2nd metatarsal and 2nd versus 5th metatarsal, where divergence (+) / convergence (-) is measured in the z plane.

DISCUSSION

Children are not “small adults” and every part of their body is in continuous anatomical and functional evolution for the entire duration of growth. According to Mosca, foot is not a joint, but a set of joints that work together during gait and upright standing position. A flexible flat foot is a combination of different deformities: valgus deformity of the hind foot, supination deformity of the forefoot in opposite directions, giving the impression that the foot is “wrung out as a towel”. Flexible flat foot is not only clinically characterized by a depression or absence of the medial longitudinal arch, but also has a convex medial – plantar border, a concave lateral border. It appears externally rotated in relation to the leg, with the weight-bearing axis of the foot medially relative to the axis of the hind foot. Deformities present in a flat foot regard all planes (sagittal, frontal and transverse) in various degrees. Aim of the surgery is to achieve the best correction towards normal realignment with greatest amount of joint preservation, especially in children where there is potential for further growth and adaptation [35].

The pediatric foot has been extensively studied clinically and radiographically. Unfortunately, clinical evaluation of the foot permits us to quantify only the alignment of the hind foot, using the goniometer in the upright standing position, while weight bearing radiograms permit us to evaluate part of the foot joints, without any possibility to understand the 3-dimensional changes that occur after surgical correction. Until now, numerical biomechanical parameters that define a normal foot during standing and differences before and after surgical correction of the pediatric flat foot have never been proposed. For this purpose the RFM protocol, validated till now only in adults, was used [36,37].

The main differences relative to other 3D existing foot models are: the particular position of the markers on the calcaneus, the indirect calculation of references of anatomical landmarks (by calculation of the midpoint), the fact that the mid foot is considered as a rigid segment and the calculation of different planar angles. Recently, Mahaffey et al. compared the three most used 3D models for the pediatric foot, find-

ing that segmental foot kinematics is repeatable even in children. In particular, the 3D-RFM offers a balance of moderate repeatability and reasonable test-retest error, similar to the Oxford 3D Foot Model, but with information on mid foot kinematic, thus making it a useful instruments for clinical uses [38].

Definition of normality parameters

The first goal of this study was to define the parameters of normality of the pediatric foot using kinematic data at the upright standing position and during gait cycle. The use of a multi segment 3D Foot Model (3DMFM) took the actual reality of this complex part of the body into account, allowing to divide the foot into its numerous segments (Leg, Calcaneus, Mid foot, Metatarsus, Hallux) that are articulated one to the other. In fact this is what happens in real life, where the foot and its joints have a crucial role in supporting the body during the upright standing position and walking. For the majority of the studied parameters, results of the pediatric foot are super imposable with those already described by Leardini et all for the adult foot [36,37] showing few quantitative variations. During the swing phase, the standard deviation of the average values of the joint rotations was larger than that calculated during the stance phase. This is true for most of the joints on all three planes of the space. These data suggest that there is a greater variability, intrinsic in each subject, in the movement of the foot in the space between a support and the other, relative to the upright standing position. Also, information obtained by the definition of the kinematic data in children with clinically normal feet, permits us to state that teenagers foot is practically equal to adults, even if growth still proceeds and offers the opportunity to differentiate numerically a pathological foot from a healthy one.

Comparison between normality, before and after surgery

The results obtained from the comparison of flatfoot before, after surgery and normality, highlight important differences of the majority of variables studied, in all 3 planes.

As shown by the current kinematic analysis of the different segments of the foot, flexible flat foot in children is different than normal one, but also, its surgical correction by subtalar arthroroeisis brings foot into normality. The present investigation quantified these modifications.

The main differences regard:

- the hind foot (Sh-Ca), frontal plane, that can be clinically measured with a goniometer;
- the Chopart Joint (Ca-Mi), transverse plane, that can be clinically observed, but that is impossible to be measured; radiographically it can be measured by the talo navicular coverage angle;
- the Lisfanc Joint (Mi-Me), frontal and transverse planes, that can be observed only clinically, but that cannot be measured;
- the ratio between 1st and 2nd metatarsal bones, transverse plane, that cannot be observed clinically and radiographically;
- 2nd and 5th metatarsal bones versus ground respectively, sagittal plane, that cannot be evaluated clinically or radiographically;

- the MLA, transverse plane, clinically impossible to be evaluated, accessible to radiographical analysis using the calcaneal pitch and Meary's angle.

All these variables normalized after surgical correction of the foot, suggesting that surgery performed at the hind foot, not only corrects it, but also improves pronation of the mid foot, increases the medial longitudinal arch and improves the ratio between metatarsal bones. The method allows us to better quantify changes that clinical and radiological evaluations cannot provide.

Regarding the other variables for which no difference between flexible flat foot and normality was found, or for those in which surgery has not reported the foot to normality, further investigation is needed. One clinical explanation is that the specific type of surgery used in the current study cannot normalize all pathologies. The good patient's compliance and the reduced biological and monetary costs of the described method suggest its possible use for other surgical treatments.

Together with the clinical assessments, the current study provided a first set of data relative to foot joint rotations and planar angles of normal children. Data were used to define the range of normality in the specific age group of young adolescents. Further data collections are necessary to expand the reference values to other age ranges. Indeed, we demonstrated a good repeatability of the 3-D RFM protocol in pediatric subjects, who are characterized by a foot, which is smaller than the adult one. This conditions the position of epicutaneous markers that are necessarily very close together, therefore making more difficult their detection by the motion capture system. With the technology used for this study (6 cameras and markers of 10 mm in diameter) the minimum size of the foot, underneath of which the display of the markers is not ideal, are those relating to the shoe number 36 (EU); those with smaller feet of this measure are therefore excluded from the study and that represent a limit for the use of this specific 3D foot model. In case of important perspiration of the foot, frequently observed in case of neurological foot diseases, markers may detach from the skin giving false results of the 3-D RFM; choosing the right double-side tape, this limit could be almost completely eliminated.

CONCLUSIONS

This study confirmed that the kinematics of the ankle joint (Sh-Fo), studied with the standard gait analysis, is a simplification of the complex movements obtained by the contributions made by the other intrinsic foot joints (Sh-Fo, Ca-Mi, Mi-Me, Ca-Me). The pediatric foot is similar to the adults and flexible flat foot in children could be corrected surgically even if it is painless.

Further studies are necessary to better understand differences between flexible flat foot and normal foot as well as modifications that occur after its surgical correction by subtalar arthrodesis. For this reason, the increment of the number of the subjects may allow us to better assess the 3D modifications of the different segments of the foot, preventing outliers' influence on the statistical results, and validating the results obtained from this study. It would also be interesting to verify data obtained by the other 3D foot models for the pediatric foot, for example the Oxford foot model, assessing whether kinematic data of the

foot before and after surgery are similar. Additionally, it could be useful to evaluate the exact kinematic modifications of the foot using the various types of screws (absorbable or not) used for the subtalar arthrodesis, helping us to choose the best one.

Finally, based in my results I believe that information obtained by the kinematic data of the 3D- RFM model in children can be utilized as a supplement to static radiographic and clinical measures.

REFERENCES

1. Borelli GA. *On the movements of animals*. Springer-Verlag; 1989
2. Weber W, Weber E. *Mechanik der Menschlichen Gehwerkzeuge*. Dieterich: Gottingen; 1836
3. Marey EJ. *La machine animal. Locomotion Terrestre et aérienne*. Germer-Bailliere; 1873
4. Muybridge E. *Animal locomotion*. University of Pennsylvania, Philadelphia; 1887
5. Braune W, Braune W, Fischer O. *The human gait*. Springer-Verlag, 1987
6. Baker R. *The history of gait analysis before the advent of modern computers*. Gait Posture 2007; 26: 331-342
7. Whittle M.W. *Gait analysis: an introduction*. 4th edition. Butterworth Heinemann: Elsevier, Oxford, 2007
8. Elftman H. *The measurement of the external force in walking*. Science 1938; 88:152-153
9. Margaria DR, Cerretelli P et al. *Energy cost of running*. Journal of Applied Physiology 1963; 18:367-370
10. Saunders JB, Inman VT, Eberhart HD. *The major determinants in normal and pathological gait*. Journal of Bone and Joint Surgery (Am) 1953; 35-A, 3:543-558
11. Perry J. *Gait analysis: normal and pathological function*. Elsevier Italia, 2005
12. Cavagna GA. *Muscolo e locomozione*. Raffaello Cortina Editore, 1988
13. Boccardi S, Lissoni A. *Cinesiologia, III volume*. Società Editrice Universo, 1984
14. Baldissera F, Bartoli E. *Fisiologia e biofisica medica*. 2^a edizione. Poletto editore, 2002
15. Fedrizzi E. *I disordini dello sviluppo motorio. Fisiopatologia, valutazione diagnostica, quadri clinici, riabilitazione*. Piccin, Milano, 2004
16. Cappelletto A. *Biomeccanica del movimento, introduzione storico-metodologica*. Atletica studi 1985; 2: 155-166
17. Pisani G. *Trattato di chirurgia del piede. III edizione*. Edizioni Minerva Medica, 2004
18. Kapandji I.A. *Fisiologia articolare, Volume 2. Arto inferiore*. Società Editrice D.E.M., Roma, 1974
19. Netter F. *Atlas of human anatomy*. 6th edition- Elsevier
20. Baker R, Robb J. *Foot models for clinical gait analysis*. Gait Posture 2006; 23(4): 399-400
21. Deschamps K, Staes F, et al. *Body of evidence supporting the clinical use of 3D multisegment foot models: a systematic review*. Gait Posture 2011; 33(3): 338–349
22. Mayers KA, Wang M, et al. *Validation of a multisegment foot and ankle kinematic model for pediatric gait*. IEEE Trans Neural Syst Rehabil Eng 2004, 12(1):122–130.
23. Wright CJ, Arnold BR et al. *Repeatability of the modified Oxford foot model during gait in healthy adults*. Gait Posture 2011; 33 (1): 108-112
24. Saraswat P, MacWilliams BA, et al. *A multi-segment foot model based on anatomically registered technical coordinate systems: method repeatability in pediatric feet*. Gait Posture 2012; 35: 547–555

25. Deschamps K, Staes F, et al. *Repeatability in the assessment of multi-segment foot kinematics*. Gait Posture 2012;35: 255-260
26. Cervesi P, Pedotti A et al. *Kinematic models to reduce the effect of skin artefacts on marker-based human motion estimation*. Journal of Biomechanics 2005;38 (11):2228-2236
27. Della Croce U, Leardini A, et al. *Human movement analysis using stereophotogrammetry. Part 4. Assessment of anatomical landmark mislocation and its effects on joint kinematics*. Gait Posture 2004; 21(2): 226-37
28. Nester C, Jones RK, et al. *Foot kinematics during walking measured using bone and surface mounted markers*. Journal of Biomechanics 2007; 40(15): 3412–3423
29. Bordelon RL. *Hypermobile flatfoot in children. Comprehension, evaluation and treatment*. Clinical Orthopedic and Related Research, 1983;181:7-14
30. El O, Akcali O, et al. *Flexible flatfoot and related factors in primary school children: a report of a screening study*. Rheumatology International Journal 2006;26: 1050-1053
31. Lin CJ, lai KA, et al. *Correlating factors and clinical significance of flexible flatfoot in preschool children*. Journal of pediatric Orthopedics 2001;21:378-382
32. Feiffer M, Kotz R, et al. *Prevalence of flatfoot in preschool aged children*. Pediatrics 2006;118:634-639
33. Mac Williams BA, Cowley M, et al. *Foot kinematics and kinetics during adolescent gait*. Gait Posture 2003; 17: 214–224
34. Sraswat P., Mac Williams B.A., et al.. *Kinematics and kinetics of normal and planovalgus feet during walking*. Gait Posture 2014; 39:339-345
35. Yi-Fen SHIH, Chao-Yin Chen, et al. *Lower extremity kinematics in children with and without flexible flatfoot: a comparative study*. BMC Musculoskeletal Disorders 2012;13:13-31
36. Mosca VS. the child's foot: principles of management(editorial). Journal of pediatric Orthopedics 1998;18:281-282)Leardini A, Benedetti MG, et al *Rear-foot, mid-foot and fore-foot motion during the stance phase of gait*. Gait Posture 2007; 25(3): 453–62
37. Portinaro N, Leardini A et al. *Modifying the Rizzoli foot model to improve the diagnosis of pes planus: application to kinematics of feet in teenagers*. Journal of Foot and Ankle Research 2014; 7: 57
38. Mahaffey R., Morrison S., et al. *Evaluation of multisegmental kinematic modeling in the pediatric foot using three concurrent foot models*. Journal of Foot and Ankle Research 2013; 6:43